



UNIVERSIDADE D  
COIMBRA

Guilherme António Duarte Oliveira

**PERCEPTUAL DECISION IN VISION: STUDY  
OF CORTICAL MECHANISMS IN THE VISUAL  
INTERPRETATION OF AMBIGUOUS STIMULI**

**Dissertação no âmbito do Mestrado em Engenharia Biomédica  
orientada pelo Doutor Gabriel Nascimento Ferreira da Costa e  
pela Doutora Maria José Braga Marques Ribeiro apresentada à  
Faculdade de Ciências e Tecnologia da Universidade de Coimbra.**

Setembro de 2022





FACULDADE DE  
CIÊNCIAS E TECNOLOGIA  
UNIVERSIDADE DE  
**COIMBRA**

Guilherme António Duarte Oliveira

# **Perceptual decision in vision: study of cortical mechanisms in the visual interpretation of ambiguous stimuli**

Thesis submitted to the Faculty of Science and Technology of the University of Coimbra for the degree of Master in Biomedical Engineering with specialization in Biomedical Instrumentation

Supervisors:

Dr. Gabriel Nascimento Ferreira da Costa

Dr<sup>a</sup>. Maria José Braga Marques Ribeiro (FMUC and CIBIT-ICNAS, UC)

**Coimbra, 2022**

This work was developed in collaboration with:

**ICNAS - Institute of Nuclear Sciences Applied to Health**



**CIBIT - Coimbra Institute for Biomedical Imaging and Translational  
Research**





Esta cópia da tese é fornecida na condição de que quem a consulta reconhece que os direitos de autor são pertença do autor da tese e que nenhuma citação ou informação obtida a partir dela pode ser publicada sem a referência apropriada.

This copy of the thesis has been supplied on condition that anyone who consults it is understood to recognize that its copyright rests with its author and that no quotation from the thesis and no information derived from it may be published without proper acknowledgement.

# Agradecimentos

Começo por dirigir uma palavra de agradecimento ao Gabriel Costa, uma pessoa com uma fome insaciável de conhecimento, por todo o seu apoio ao longo desta etapa, por sempre ter acreditado no potencial deste projeto e acima de tudo pela disponibilidade constante. Agradeço também à Maria Ribeiro sem a qual este projeto não seria possível, cujo o rigor e brio profissional foram essenciais para a qualidade do trabalho que apresento aqui.

Aos vinte e sete voluntários que aceitaram contribuir para esta tese, um muito obrigado, a realização deste projeto não teria sido possível sem a vossa paciência e vontade de ajudar.

Para todos aqueles que de alguma forma me marcaram durante estes 5 anos em Coimbra e aos meus amigos em Viseu, agradeço do fundo do coração. Sem o vosso apoio e sem o vosso contributo, a minha vida teria sido sem sombra de dúvida um caminho muito mais difícil de percorrer. Um especial agradecimento a ti Mi, etapas vão e vêm mas tu serás sempre uma constante na minha vida. Obrigado por tudo o que fazes por mim e por acreditares sempre nas minhas capacidades.

Por fim, deixo o meu maior agradecimento aos meus pais e à minha irmã por me terem acompanhado nesta jornada tão importante na vida de um jovem adulto. Obrigado pela confiança que depositam em mim e por todo o esforço que fizeram para que nunca me faltasse nada durante vinte e três anos da minha vida. Tenho a certeza que o vosso esforço não será em vão!



# Resumo

O estudo dos mecanismos neuronais por detrás das representações visuais perceptuais continua a ser um campo fascinante das neurociências cognitivas. Embora a percepção humana seja notavelmente eficiente, esta pode ser desafiada por figuras que conduzem a representações inerentemente ambíguas, mas possíveis. Nestes casos, o sistema visual tem de seleccionar uma das várias percepções ambíguas alternativas. Quando o estímulo é visualizado de forma constante, as múltiplas interpretações dominam a percepção em alternância durante breves períodos de tempo, numa situação de rivalidade perceptual. Quando a informação sensorial é consistente com apenas duas interpretações, sem informação que possa fazer convergir a percepção para uma única interpretação, o fenómeno é chamado de percepção biestável. No entanto, se estímulos ambíguos forem apresentados de forma breve o cérebro decide entre uma das interpretações com uma frequência que pode favorecer uma delas.

Uma questão particularmente intrigante recai sobre como é que a organização do córtex visual pode influenciar a percepção em condições de ambiguidade. Estímulos visuais apresentados em locais adjacentes do campo visual ativam áreas corticais adjacentes do córtex visual, com exceção de estímulos que atravessem os meridianos vertical e horizontal. Nestes casos, estímulos que são representados num espaço visual contínuo são processados em mapas corticais com descontinuidades e heterogeneidades que podem ter influência no desfecho perceptual. Para estudar a hipótese de que particularidades da topografia e arranjo do córtex visual influenciam a percepção de movimento ambíguo, utilizamos o estímulo ambíguo de Movimento Alternativo Estroboscópico (SAM). Este pode ser percebido como descrevendo movimento horizontal ou vertical com probabilidades que tanto favorecem interpretações "económicas" como são sensíveis a idiossincrasias da estrutura e conectividade cortical.

Em duas experiências, com o objetivo de estimar psicometricamente a preferência

do sistema visual por uma determinada direção de movimento, executámos um método robusto utilizando um sistema de controlo de posicionamento ocular. Ao manipular o rácio entre as dimensões (distância horizontal/vertical) do SAM, enviesámos a percepção do participante para uma direção específica, a fim de obter o rácio necessário para alcançar a percepção equiprovável do movimento aparente horizontal e vertical, chamado rácio de paridade. Na primeira experiência, esta métrica estável e específica para cada participante relacionada com o processamento do movimento visual foi estimada para 8 posições diferentes, equidistantes do centro do campo visual, para ambos os hemisférios. Isto permitiu-nos avaliar como a percepção do participante foi alterada pela posição do SAM. Uma análise envolvendo 20 participantes revelou um rácio de paridade mais elevado para os estímulos exibidos sobre o meridiano horizontal do campo visual. Um rácio de paridade mais elevado traduz uma maior tendência para perceber o movimento aparente horizontal. Com isto, pela primeira vez, foi demonstrado que existe uma tendência de percepção de movimento horizontal para estímulos ambíguos que estão posicionados no meridiano horizontal, à semelhança da tendência de percepção vertical no meridiano vertical. Este fenómeno foi observado em condições de controlo restrito da fixação visual de forma a garantir consistência na apresentação do estímulo nas regiões retinotópicas. A fim de compreender se a origem deste efeito perceptual específico poderia estar em regiões mais primárias do córtex visual, foi feita uma segunda experiência. Nesta, o rácio de paridade foi obtido para cinco estímulos colocados na mesma posição (meridiano horizontal) com diferentes contrastes visuais. Não foram observadas diferenças significativas entre os rácios de paridade medidos, o que sugere que o córtex visual primário, que é particularmente sensível a variações de contraste, pode não ter um papel nesse viés horizontal.

Os nossos resultados mostram uma consequência funcional de uma organização cortical microestrutural ou a mesoescala, nomeadamente um produto da arquitectura neuronal alinhada com direcções específicas ou uma consequência de mecanismos auxiliares necessários à integração entre áreas corticais visuais descontínuas. Por conseguinte, são necessários mais estudos psicofísicos e neurofisiológicos para esclarecer quais poderão ser as causas por detrás da tendência horizontal na percepção ambígua do movimento.

**Palavras chave:** movimento aparente biestável, meridiano horizontal, córtex visual primário, rácio de paridade.

# Abstract

The study of the neural mechanisms behind the emergence of visual perceptual representations remains a fascinating field of cognitive neuroscience. Despite that human perception of objects and scenes is remarkably efficient, it can be challenged by figures which lead to inherently ambiguous, but possible, representations. Thus, the visual system has to select one of several ambiguous alternating percepts. In other words, when the visual stimulus is constantly seen, the multiple interpretations compete for the perception's dominance, in a situation of perceptual rivalry. When the sensory information is consistent with only two interpretations, without information that may cause perception to converge on a single interpretation, the phenomenon is called bistable perception. However, if the ambiguous stimuli are quickly displayed, the human brain will choose one of the possible interpretations with a frequency that can favor that one perception or the other.

A particular intriguing question is how the visual cortex organization can influence perception in conditions of ambiguity. Visual stimuli presented in adjacent locations in the visual field activate adjacent cortical locations in early visual cortical areas, with the exception of stimuli that cross the vertical or horizontal meridians. In these cases, stimuli that are represented in a continuous visual space are processed in cortical maps with discontinuities and heterogeneities that can have an influence on perceptual outcome. In order to study the hypothesis that particularities of the topography and arrangement of the visual cortex influence ambiguous motion perception, we used the Stroboscopic Alternative Motion (SAM) ambiguous stimulus. This stimulus can be perceived as describing horizontal or vertical motion with probabilities that can both favor "economic" interpretations and be sensitive to idiosyncrasies of cortical structure and connectivity.

In two experiments, with a focus on estimating psychometrically the preference of the visual system to a particular direction of motion, we employed a robust method using an eye tracking system for strict control of gaze positioning. By manipulat-

ing the SAM's aspect ratio (horizontal by vertical distance), we biased participant's perception toward a specific direction in order to obtain the aspect ratio required to reach equiprobable perception of horizontal and vertical apparent motion, called parity ratio. In the first experiment, this subject-specific and stable metric of visual motion processing was estimated for 8 different positions in the visual field, equidistant from its center, over both hemifields. This allowed us to evaluate how the viewer's perception was altered by the SAM's position. A multi-subject analysis revealed a higher parity ratio for the visual stimuli displayed over the horizontal meridian of the visual field. A higher parity ratio traduces a greater tendency to perceive horizontal apparent motion. Consequently, our findings demonstrate, for the first time, that there is a horizontal bias for ambiguous motion perception for stimuli falling within the horizontal meridian, similar to the vertical perception bias observed in the vertical meridian. This phenomenon was observed under conditions of strict control of visual fixation in order to ensure consistency of the stimulus presentation in the retinotopic regions. In order to understand if the origin of this location-specific perceptual effect could be in the earlier regions of the visual cortex, we run a second experiment. In this one, the parity ratio was obtained for five stimulus placed in the same position (horizontal meridian) with different visual contrasts. No significant differences were obtained for the measured parity ratios, which suggests that the primary visual cortex, which is particularly sensitive to visual contrast, might not be relevant for the horizontal motion bias.

Our results suggest a perceptual bias that could be a functional consequence of microstructural or mesoscale cortical organization, namely a product of neural architecture aligned to specific directions or a consequence of ancillary mechanisms necessary for integration between discontinuous visual cortical areas. Further psychophysical and neurophysiological studies are needed to clarify what could be the causes behind the horizontal bias for ambiguous motion perception.

**Keywords:** bistable apparent motion, horizontal meridian, parity ratio, primary visual cortex.

# Contents

<b>List of Figures</b>	<b>x</b>
<b>List of Tables</b>	<b>xii</b>
<b>List of Abbreviations</b>	<b>xiii</b>
<b>1 Introduction</b>	<b>1</b>
1.1 Motivation . . . . .	1
1.2 Background . . . . .	2
1.2.1 Visual Cortex . . . . .	2
1.2.2 Ambiguity in Vision . . . . .	5
1.2.3 An Empirical Approach to Perceptual Mechanisms . . . . .	9
1.2.4 Visual motion perception . . . . .	12
1.2.5 Apparent motion . . . . .	15
<b>2 Aims of the project</b>	<b>17</b>
<b>3 Methods</b>	<b>20</b>
3.1 Participants . . . . .	20
3.2 Stimulus . . . . .	20
3.3 Ambiguous Stimuli Calibration - Procedure . . . . .	22
3.3.1 Determining individual Parity Ratios . . . . .	22
3.3.1.1 Method of Limits (MoL) . . . . .	23
3.3.1.2 Method of Constant Stimuli (MoCS) . . . . .	24
3.3.2 Visual Tasks . . . . .	25
3.4 Psychometric Function fitting . . . . .	29
3.5 Eye tracking . . . . .	31
3.5.1 Procedure . . . . .	31
3.5.2 Data Processing . . . . .	32
3.6 Statistical Analysis . . . . .	33
<b>4 Results and Discussion</b>	<b>34</b>
4.1 Preliminary Work . . . . .	34
4.2 Visual Tasks . . . . .	36
4.2.1 Experiment 1 . . . . .	36
4.2.1.1 Eyetracking Analysis . . . . .	40



4.2.2	Experiment 2 . . . . .	43
4.3	General Discussion . . . . .	46
<b>5</b>	<b>Conclusion and Future perspectives</b>	<b>50</b>
	<b>Bibliography</b>	<b>52</b>
<b>A</b>	<b>Appendix</b>	<b>65</b>

# List of Figures

1.1	Visual field maps in human visual cortex. . . . .	3
1.2	Retinotopic organization of the human visual cortex. . . . .	5
1.3	Cortical magnification of the primary visual cortex (V1) visual field map. . . . .	5
1.4	Visual multistable phenomena examples. . . . .	8
1.5	Discrepancies between luminance and perceptions of lightness and brightness. . . . .	10
1.6	Similar surfaces under similar illuminations (left) and different surfaces under different illuminations (right). . . . .	10
1.7	Simultaneous color contrast stimulus. . . . .	12
1.8	Color contrast and constancy effects produced by empirical generation of visual perceptions. . . . .	12
1.9	Physical motion processing pathway. . . . .	13
1.10	Location of the human Middle Temporal complex (hMT+). . . . .	14
1.11	Apparent vertical motion. . . . .	16
3.1	Stroboscopic Ambiguous Motion (SAM) stimulus. . . . .	21
3.2	Method of Limits (MoL). . . . .	23
3.3	Psychometric Function. . . . .	24
3.4	Stroboscopic Alternative Motion (SAM) phases used in the Method of Limits (MoL). . . . .	26
3.5	Stroboscopic Alternative Motion (SAM) positions used in the Method of Constant Stimuli (MoCS). . . . .	28
3.6	Infrared oculographic eye tracker. . . . .	32
4.1	Percentage of vertical motion perception for all participants per stimulus position. . . . .	36
4.2	Psychometric function and respective interpolated parity ratios for left and right hemifields of participants 03, 06 and 14. . . . .	38
4.3	Distribution of parity ratios for all participants per stimulus position. . . . .	39
4.4	Average fixation density plots for the left and right hemifields of participants 03, 06 and 14. . . . .	41
4.5	Distribution of the parity ratio's values for all 14 participants per stimulus position. . . . .	43

---

4.6	Psychometric functions (left) and respective interpolated parity ratios (right) for the left hemifield of participants 02 and 21 and right hemifield of participant 22. . . . .	45
4.7	Distribution of the parity ratio's values for all participants per Michelson contrast independently of the hemifield. . . . .	46
A.1	Psychometric functions for the left hemifield of all participants in experiment 1. . . . .	66
A.2	Psychometric functions for the right hemifield of all participants in experiment 1. . . . .	67
A.3	Average fixation density plots for the left hemifield all participants. . . . .	68
A.4	Average fixation density plots for the right hemifield all participants. . . . .	69
A.5	Psychometric functions for all participants in experiment 2 . . . .	70

# List of Tables

3.1	Method of Constant Stimuli (MoCS) data. . . . .	24
4.1	Percentage of vertical motion perception of participants 03, 06, 14 as well as the average for all participants, for each position used in the visual stimulus of the left hemifield. . . . .	37
4.2	Percentage of vertical motion perception for participants 03, 06, 14 as well as the average for all participants, for each position used in the visual stimulus of the right hemifield. . . . .	37
4.3	Average parity ratios for the middle, top and bottom positions of the left hemisphere, for both the original and the fixation controlled psychometric functions. . . . .	42
4.4	Average parity ratios for the middle, top and bottom positions of the right hemisphere, for both the original and the fixation controlled psychometric functions. . . . .	42
4.5	Percentage of vertical motion perception values for participants 02, 21 and 22 as well as the average for all participants, for each Michelson contrast used in the visual stimulus. . . . .	44

# List of Abbreviations

- AM** Apparent motion. 15
- FC** Fixation Controlled. 42
- fMRI** functional Magnetic Resonance Imaging. 12, 43, 50, 51
- hMT** human Middle Temporal area. 13, 14
- hMT+** human Middle Temporal complex. 13, 14, 15, 17, 18
- IPS** Intraparietal sulcus. 3, 13
- ISI** Inter Stimulus Interval. 18, 21
- ITC** Inferior Temporal Cortex. 4
- ITI** Inter Trial Interval. 27
- ITS** Inferior Temporal Sulcus. 14
- LGN** Lateral Geniculate Nucleus. 3, 13
- LO** Latero-occipital cortex. 3
- MC** Michelson Contrast. 28, 43, 44
- MoCS** Method of Constant Stimuli. 20, 21, 24, 25, 27, 34, 36, 38, 43, 44, 66, 67, 70
- MoL** Method of Limits. 20, 21, 23, 24, 25, 26, 27, 36, 44
- MST** Medial Superior Temporal area. 13, 14
- PPC** Posterior Parietal Cortex. 4
- PR** Parity Ratio. 22, 23, 26, 27, 29, 35, 36, 37, 39, 40, 42, 43, 44, 46, 48
- SAM** Stroboscopic Alternative Motion. 1, 2, 17, 18, 19, 20, 21, 22, 26, 27, 31, 34, 46, 47, 48, 50
- SE** Standard Error. 30
- SEM** Standard Error of the Mean. 35, 36, 37, 39, 42, 44, 46
- SFM** Structure From-Motion. 6
- STS** Superior Temporal Sulcus. 14
- TMS** Transcranial Magnetic Stimulation. 18
- V1** primary visual cortex. x, 2, 3, 4, 5, 13, 14, 15, 46, 49, 50

# Introduction

## 1.1 Motivation

The human brain constantly interprets different stimuli from the environment around it, based on incomplete or ambiguous information. This task is particularly evident in vision. In multiple situations, it is necessary to interpolate information that is frequently missing as well as to decide between multiple valid interpretations.

When the sensory information is ambiguous and consistent with two exclusive interpretations, in the absence of information that could make perception converge to only one interpretation, a phenomenon called bistable perception can occur. This is characterized by spontaneous perceptual reversals that occur every few seconds between the two possible interpretations [1]. The Stroboscopic Alternative Motion (SAM) or “motion quartet” is an apparent motion stimulus that vividly exemplifies such phenomenon. A SAM consists of two flashing dots displayed simultaneously on diagonally opposite corners of a virtual rectangle, which are subsequently switched off and replaced by two dots appearing on the other two corners. This leads to periods of horizontal or vertical motion perception that alternate in a stochastic manner.

The quantitative relationship between the stimulus physical properties and its subjective perception is given by psychophysics. In the case of SAM, multiple factors can influence one’s perception such as the distance between the dots, the rate at which they switch on and off or their contrast [2–6]. However, a stimulus’ perception might not only be influenced by its physical properties but also by biases of the sensorial system and anatomical constraints of the human brain. In fact, it is well established that observers are more likely to perceive vertical than horizontal motion when the SAM is presented centrally in the visual field. This asymmetry has been attributed to the fact that perception of horizontal motion requires integration across the brain’s hemispheres whereas perception of vertical motion requires only intrahemispheric processing [7].

Preliminary studies using the SAM revealed a similar effect happening within the hemisphere, in which observers are more likely to perceive horizontal than vertical motion when the stimulus crosses the horizontal meridian of the visual field. This effect might be supported by the strong correlation between contingencies in cortical folding (gyri and sulci) and brain function, cognition, and behaviour. In this matter, it has been long known that much of the primary visual cortex (V1) is located within a deep furrow, named the calcarine sulcus, and that the tight spatial linkage between the fundus of this sulcus and the representation of the horizontal meridian appears to be specific to human brains [8].

Knowing this, the current study aims to better understand the way the human brain interprets visual stimuli and relate it with its anatomical constraints. In particular, whether ambiguous stimulus falling within specific regions of the visual cortical map are more frequently perceived in a particular configuration and, thus, influence its apparent motion perception. This could be explained by influences of the calcarine sulcus deformation or other visual cortical map contingencies that affect perception of motion across the horizontal midline.

## 1.2 Background

### 1.2.1 Visual Cortex

The visual cortex is the primary cortical region of the brain responsible for receiving, integrating and processing the visual information. This area is in the most posterior region of the brain, includes the entire occipital lobe and extends significantly into the temporal and parietal lobes, spanning about 20% of cerebral cortex [9]. Each hemisphere has its own visual cortex, which receives information from the contralateral visual field, and can be divided into over thirty different areas based on its structure and function, of which we can highlight: V1, also known as striate or primary visual cortex, and extrastriate cortex composed of V2, V3, V4 and V5. These sub regions are arranged hierarchically in an anterior to posterior order, with simple visual features represented in 'lower' areas, i.e. more posterior, and more complex features represented in 'higher' areas, i.e. more anterior. In other words, as information gets passed along, each subsequent cortical area is more specialized than the last [10], displaying neurons with more complex receptive fields and sensitivity to different stimulus features. Over the years, several 'higher' areas (figure 1.1) have been described beyond the ones mentioned above, showing specialization for complex aspects of visual scenes such as recognition of objects, words and faces [9].

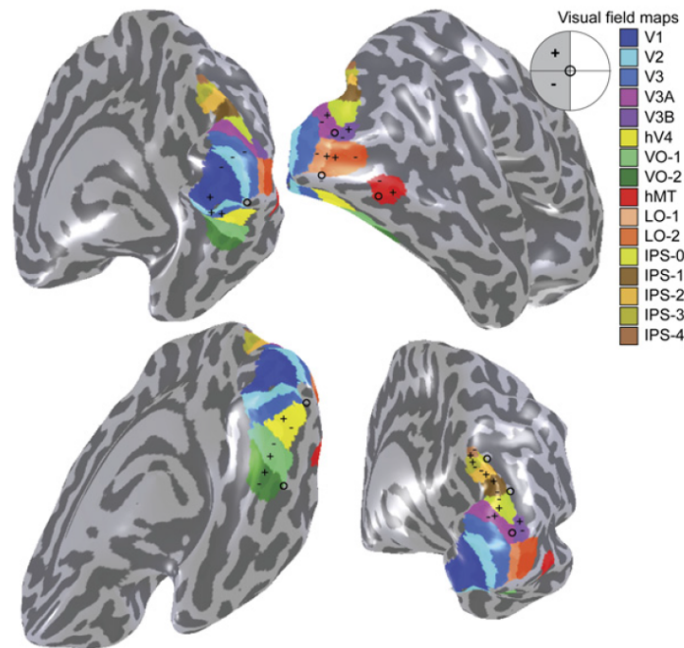


**Figure 1.1: Visual field maps in human visual cortex.** The positions of sixteen maps are shown on an inflated representation of the cortical surface of the human’s brain right hemisphere. Fovea and upper/lower visual fields are indicated by the “o”, “+” and “-“ symbols, respectively. V1 corresponds to the primary visual cortex or striate cortex, while V2, V3 and more posterior areas are the extrastriate cortex. The hMT is the human middle temporal area, also referred to as V5. The Latero-occipital cortex (LO) and Intraparietal sulcus (IPS) perform more specialized functions in object vision and in representations of visual space, respectively. Reproduced from [9].

When visual data is sent forward from the retina, it travels through the optic nerve to the Lateral Geniculate Nucleus (LGN) of the thalamus and then is relayed to the first area of the visual cortical hierarchy, the striate cortex. The striate cortex (V1) is composed by six distinct layers, each comprising different cell-types and functions. Layer four is the main input layer, which receives information from the LGN and where can be found the highest number of simple cells (cells that respond to specific types of visual cues such as the orientation of lines) with a small spatial and functional receptive field. This specific 6-layered organization is not exclusive of the visual cortex, but in fact corresponds to a canonical arrangement of all mammalian cortex [11]. Neurons in the primary visual cortex are sensitive to very basic visual signals, displaying oriented receptive fields that respond accordingly to oriented stimuli such as a contrast defined bars and also to oriented motion within a small aperture [12]. In humans, V1 neurons are organized in columns with similar preferred orientation spanning the entire thickness of the cortex. For instance, neurons in one column may respond to stimuli which have a vertical orientation while the neurons in



a different column may respond primarily to horizontal orientation. These neurons columns are grouped to form assemblies known as modules, required to analyse a particular region of the visual field [10] [1].

Moving up the visual hierarchy, V2, which receives feedforward signals from and sends feedback signals to V1, integrates information from V1 and thus can display higher level of complexity and reaction patterns to visual stimuli. Researchers have recorded cells in this region responding to differences in color, spatial frequency and combined orientations [13], thus closer to object-like features. Afterwards, visual signals are sent from V2 to more anterior regions in two different pathways, which are specialized in different aspects of the visual information processing. The ventral stream goes through ventral V3, V4 and the Inferior Temporal Cortex (ITC), and is associated with object recognition. The dorsal stream goes through areas dorsal V3, V5 and to the Posterior Parietal Cortex (PPC), and focuses on spatial processing and visual-motor skills [10].

The visual data processing is highly specialized and allows the brain to recognize objects and patterns with no conscious effort. One advantage of this specialization is that other cortical regions are free to, in parallel, perform other computations such as executive functions and decision making [10]. However, despite its capacity to parse and combine information quickly between several dedicated visual areas, the visual brain is still susceptible to misinterpretation of visual data. This can be demonstrated by the efficacy of visual illusions [14].

Throughout the visual pathway, as cortex interprets different aspects of the visual image, the cortical circuitry is organized using receptive fields that preserve the most critical image information, its spatial organization. Hence, regions of visual cortex with a variety of visual functions still preserve the visual field map or retinotopic map [9] (figure 1.2).

The retinotopic map provides useful information about the likely perceptual function of a specific cortical region. For example, field maps define the amount of cortical surface area as a function of visual field eccentricity, a measure called cortical magnification [9] (figure 1.3). Some cortical visual field maps are mainly devoted to processing foveal information while others less so [15–17]. Such variability in cortical magnification may correlate with differences in perceptual processing requirements [18].

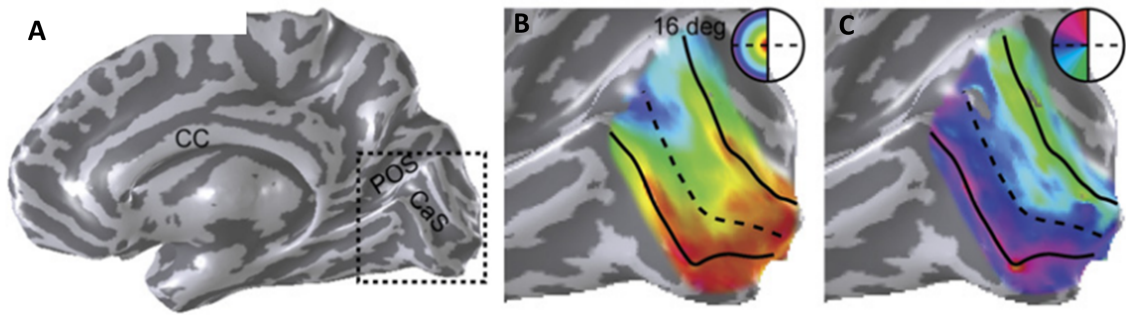


**Figure 1.2: Retinotopic organization of the human visual cortex.** Inflated cortical surface of the human’s brain right hemisphere (A) with CC as corpus callosum, POS as parietal-occipital sulcus and CaS as calcarine sulcus (dashed lines in figures B and C). An expanded view near the calcarine sulcus is overlaid with a color map of eccentricity (B) and visual angle (C) – see colored legends. Reproduced from [9].

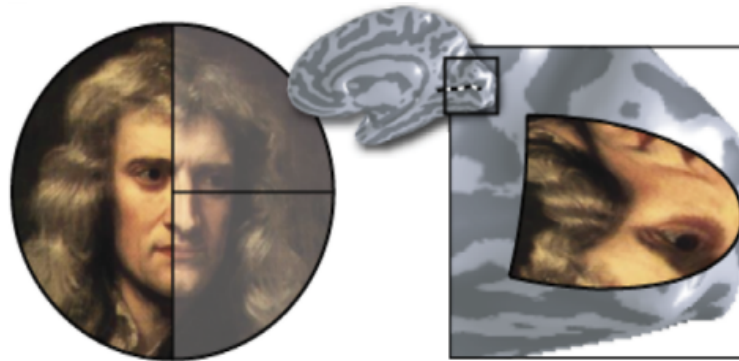


**Figure 1.3: Cortical magnification of the V1 visual field map.** Illustration of how the visual field (left) is transformed and represented on the V1 cortical surface (right): the image is inverted, and the centre of the visual field is greatly expanded (cortical magnification). Reproduced from [9].

## 1.2.2 Ambiguity in Vision

Perceptual resolution of ambiguity is fundamental for seeing as visual perception is essentially an ambiguity solving process. In fact, most of us are unaware of what a challenging effort our brain is doing since our visual system is so effective at creating an accurate image of the real world. Our visual system absorbs and decodes complicated information automatically, giving us a coherent perception of our surroundings. Despite that, our perceptions are not always perfect as sometimes our brain will interpret a static image on the retina in more than one way. Because a significant portion of object information is either not encoded or confused with other elements of the visual scene, retinal images do not provide complete, exact information about physical agents [19]. This creates ambiguity about the objects in view since different physical objects can generate an identical retinal image, and

conversely, a single object can deliver an infinity of different images to the eye depending on, for example, viewing angle, distance and illumination [19]. To resolve those ambiguities, the nervous system is forced to rely on data that is encoded in previous experiences, expectations, context, and in the motor activity of the individual who is trying to perceive something in the visual world. Accordingly, based on the evidence from these several sources of information, the nervous system must make a perceptual decision about the most likely state of the world [20].

Perception of our three-dimensional world is based on two-dimensional optical projections that fall on the retina of each eye. This means that the retrieval of all the visual information about the three-dimensional environment from the very limited information contained in the two-dimensional retina image is a process inherently ambiguous as some information is inevitably lost. In other words, neural processes act on the retinal image in the process of creating perception as imperfect information at an initial encoding stage is followed by perceptual representations that are extrapolated from the incomplete retinal data [19].

The occurrence of multiple competing interpretations of visual input, i.e., visual multistability, provides ways to study the processes of ambiguity resolution. Multiple examples of visual multistable phenomena are depicted in figure 1.4. When faced with ambiguity or visual conflict, the brain analyzes data supporting several, competing explanations about what is being observed and, when that evidence is not strong enough to rule out all but one interpretation, we become consciously aware of the alternative solutions. In fact, many aspects of visual multistable perception are consistent with the notion of perception as inference based on various sources of information. To give some examples:

- When, during multistable vision, the reliability of the evidence supporting one interpretation is higher than that of the evidence that favors another, perception is biased toward the former one. Thus, during binocular rivalry, a form of multistable perception triggered when two eyes see different monocular stimuli (figure 1.4.C), the perceptual experience of the observer favors a well-focused monocular stimulus over a blurred one [21]. Likewise, an ambiguous Structure From-Motion (SFM) animation (figure 1.4.D) is more often observed to rotate in a given direction when additional visual information, such brightness disparity, associated with that direction is introduced to the display [22].
- When seeing a multistable display in conjunction with stimulus information from another nonvisual sensory input, this auxiliary information can increase the preponderance of the visual interpretation that is congruent with the non-visual stimulus. There have been reports of these accessory multisensory inter-

actions for multistability generated by an ambiguous facial image paired with unambiguous voices [23] and by ambiguous apparent motion stimuli complemented by tactile motion [24].

- Frequently, perceptual dominance favors the interpretation suggested by the behavioral context when one visual interpretation is more compatible with it than another perception is [25]. Take the example, in binocular rivalry, of two globes rotating in the same manner and presented monocularly with only one being under the participant's control. In this case, the self-controlled globe will be more frequently dominate perception than the behaviorally irrelevant globe [26].
- Expectations and past experiences both have an impact on multistable perception. When observers are exposed to the same ambiguous stimulus repeatedly, perception upon each presentation of the stimulus strongly tends to match the perception on the previous presentation [27, 28]. Similarly, prior exposure to an unambiguous stimulus can also significantly influence perception of ambiguous stimuli [29, 30]. In addition, it is widely known that acquired expectations, both implicit and explicit, can affect how perceptually ambiguous inputs are interpreted [31–33].

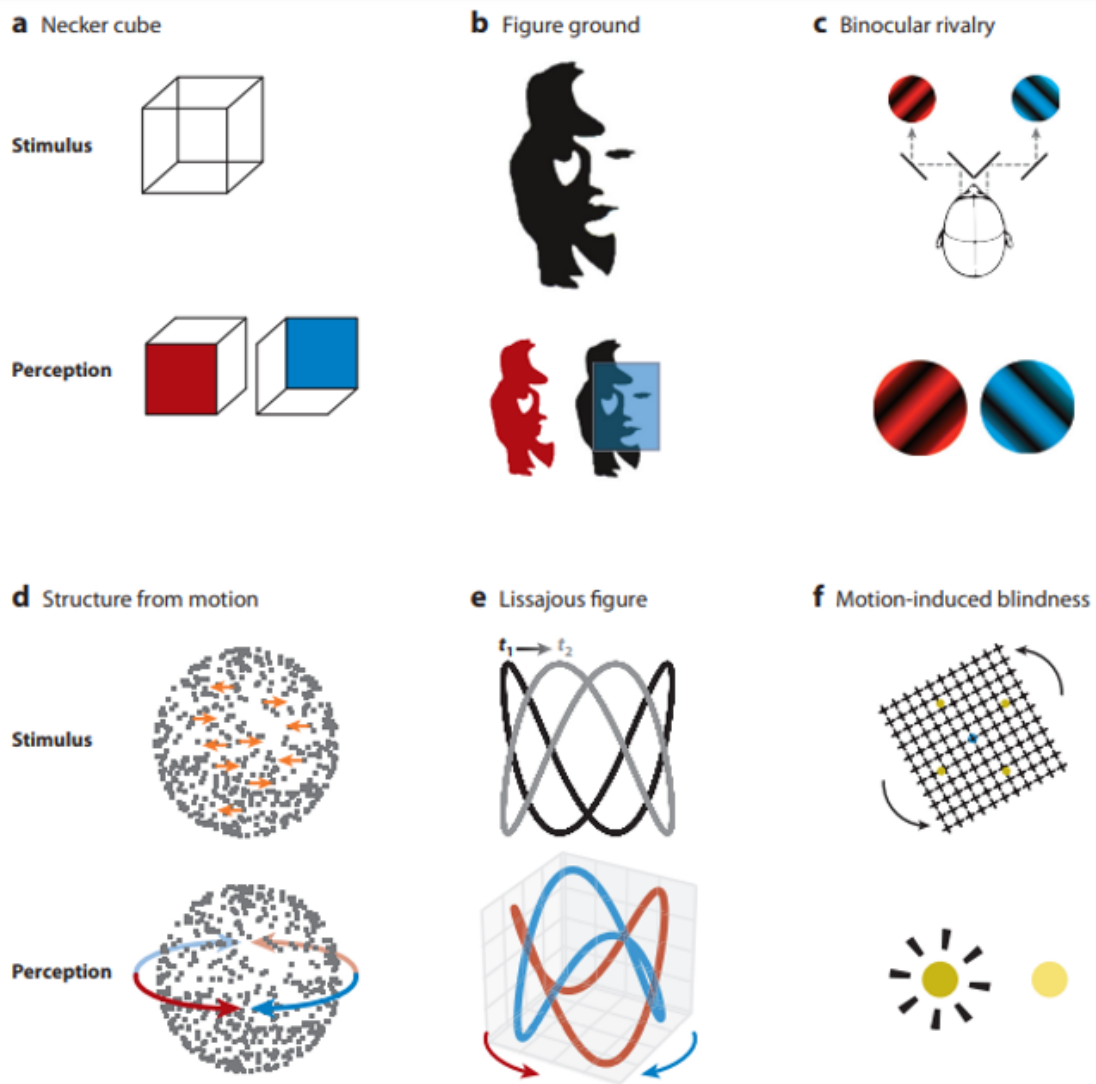


**Figure 1.4: Visual multistable phenomena examples.** All stimuli above are depicted with the original stimulus on top and the competing percepts that result from it below. A) The Necker cube is ambiguous in terms of the three-dimensional geometry it represents. Two different cube faces can be perceived as the forward-facing side of the cube. B) Ambiguities in figure–ground assignment promote alternative interpretations of the pictorial content, which, in this stimulus, can correspond to either a saxophone player or a woman’s face. C) Binocular rivalry takes place when the two eyes view dissimilar monocular images. D) Structure-from-motion. When the projection of a sphere of dots is presented orthographically, depth order is ambiguous, and the sphere can be seen to rotate with the front-surface dots moving either leftward or rightward. E) Lissajous figures are also ambiguous structure-from-motion stimuli. When viewing this stimulus, transitions between the perceptual interpretations of the nearest line segment moving left or right are temporally confined to moments of self-occlusion. F) Motion-induced blindness occurs when static stimuli (yellow circles) are presented near a moving surface. The static stimuli periodically disappear from the viewer’s awareness. Taken from [20].

### 1.2.3 An Empirical Approach to Perceptual Mechanisms

The examples highlighted in the previous section made clear that the information contained in the retinal image cannot accurately identify the real sources of the stimulus in the physical world. As a result, there is inherent uncertainty in the relationship between the environment and the way we perceive it. Therefore, to surpass this biological dilemma, the human visual system uses feedback from the success or failure of past behavioural responses to the various visual stimuli in the environment, to progressively instantiate patterns of neural connectivity that promote even more useful reactions to those stimuli in the future. Rather than analyzing the components of the retinal image as such, percepts are determined probabilistically [34]. In this section, two examples of this phenomena will be given.

#### **The relationship between luminance and brightness**

A corollary is that objects in a scene emitting the same amount of light to the eye should appear to be equally bright or light [35]. Nonetheless, perceptions of lightness (appearance of objects due to the quantity of light that their surfaces returns to the eye) and brightness (appearance of objects that are themselves sources of light), fail to meet these assumptions. For example, two regions with the same luminance are perceived as being differently light or bright when their backgrounds have distinct luminance values (figure 1.5.A) [36]. Furthermore, as has already been documented [37], displaying luminance areas in more complex contexts makes this effect much stronger (figure 1.5.B).

Since the amount of light reflected to the eye from any area of a scene relies on both the illumination and reflectances of the pertinent surfaces, the equiluminant returns from the targets regions in figure 1.5.A are intrinsically ambiguous. Such stimuli can be generated by surfaces that reflect light identically under the same illumination (figure 1.6-left), or by differently reflective surfaces under distinct amounts of illumination (figure 1.6-right) [34]. It has been proposed that this uncertainty can be resolved using feedback from the success or failure of prior behavioral responses to the same sort of stimulus [36]. Therefore, target areas will tend to appear similarly bright as long as the stimulus is compatible with prior observations of similarly reflecting target surfaces under the same illumination. In the same way, if the stimulus is consistent with the experience of differently reflecting objects at distinct illumination levels, the target regions tend to appear differently bright. Since the visual information in the standard stimulus for brightness contrast (figure 1.5.A) is consistent with both different surfaces under different illuminations and similar surfaces under similar illuminations, then the observer's perception will reflect both

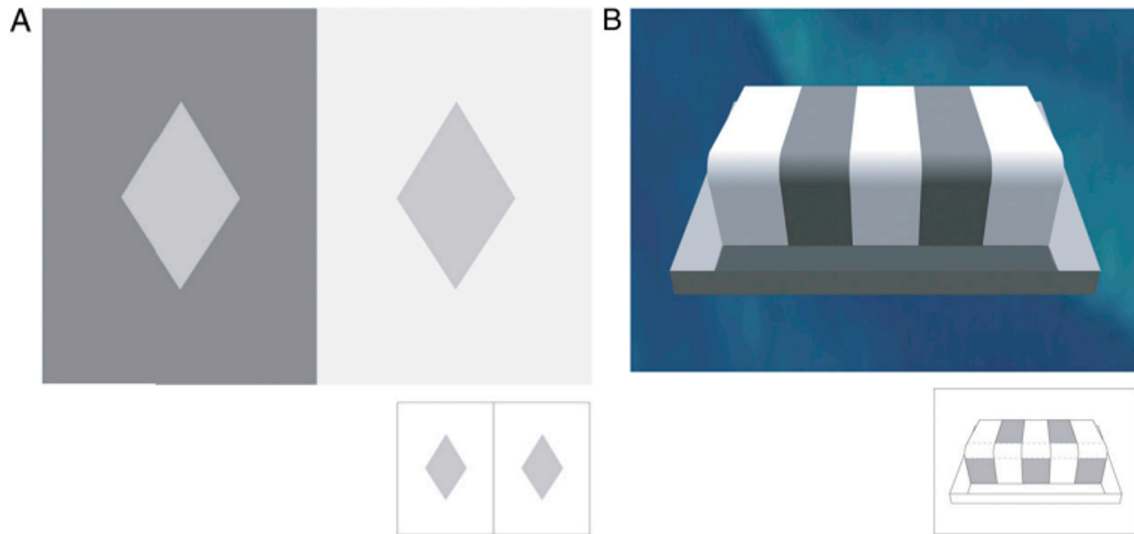


**Figure 1.5: Discrepancies between luminance and perceptions of lightness and brightness.** A) Simultaneous brightness contrast effect. The same gray area (same measured luminance) is perceived as being lighter or brighter in a darker surround than in a lighter one. B) The same effect observed in A) where a perceptual disparity in lightness is generated by contextual information that one set of patches is in shadow (on the riser of the step) while the other is in light (on the surface of the step). Taken from [35].

possibilities [34]. According to an empirical or predictive hypothesis of perception, the continuous experiencing of the world and learning during development leads priors that guide perception based on how frequently specific conditions are met in the real world. This can explain, for instance, priors of interpreting illumination coming from above. Other luminance based illusions might rely on more hardwired mechanisms such as surround-suppression (1.6, dots on top of tables).

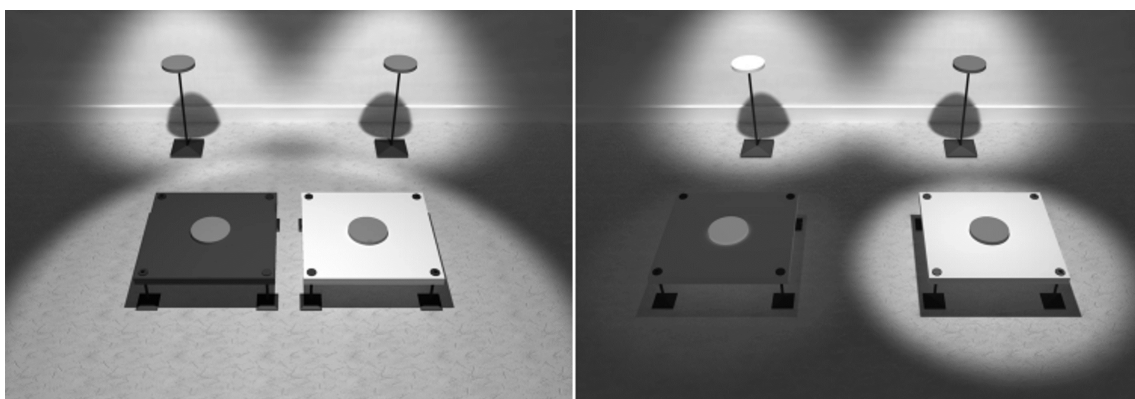


**Figure 1.6: Similar surfaces under similar illuminations (left) and different surfaces under different illuminations (right).** Taken from [36].

### The relationship between spectral returns and colour

The distribution of spectral power in a light stimulus, which is what causes color

perceptions, is ambiguous for exactly the same reasons as is the overall spectral intensity. Illumination, reflectance and other factors that modulate the properties of the light that enters the eye are inextricably linked in the retinal image. As in the brightness contrast effect already explained, two targets with the same spectral composition placed on differently colored backgrounds can look different but now in terms of their respective color qualities (figure 1.7) [36]. In the past, this phenomenon was described as the adaptation of the color system to the average spectral content of the overall stimulus [38–40]. Nonetheless, these schemes fail to account for the fact that color contrast stimulus can be crafted to elicit different color percepts despite having the same average chromatic surrounds [41]. However, an explanation for this stimulus can be given in empirical terms as the percept elicited by it can be determined by the relative frequencies of occurrence of the real-world combinations of reflectances and illuminations that gave rise to that distribution of spectral power in the past [34, 36]. In other words, a spectrum stimulus should cause a sensation that includes every possible underlying source in proportion to how frequently those sources have previously occurred in human experience. The same justification can be applied to color constancy, a related phenomena where the same object continues to seem identical in color even when illuminated by different light sources. As we can verify in figure 1.8, it is possible to generate color contrast and constancy effects by empirical, probabilistic manipulation of the information in the scene [34]. In both yellowish and bluish illumination images, it is possible to make tiles on the cube’s surface that are, in a neutral context, the same shade of gray appear either blue or yellow, respectively. Contrarily, by altering the probability of their sources, it is possible to make tiles look the same color even though they are differently colored in a neutral setting. Therefore, if perceptions of color contrast and constancy can be produced in this manner, the same spectral target on two differently chromatic backgrounds (figure 1.7) is expected to result in distinct chromatic sensations.



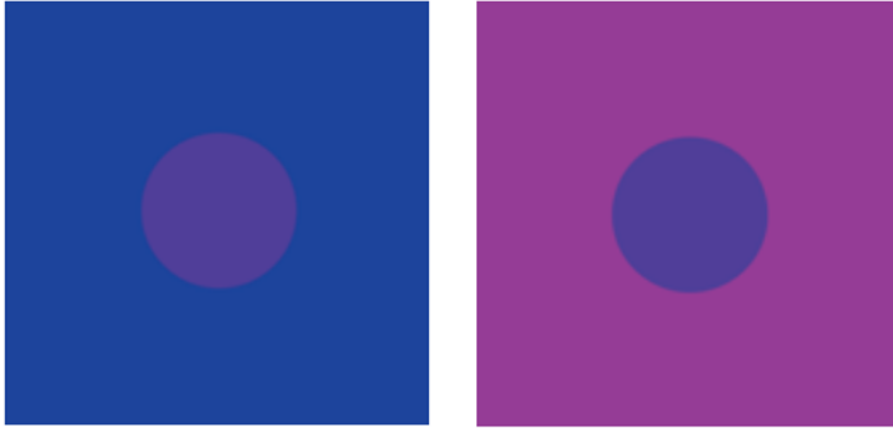


**Figure 1.7: Simultaneous color contrast stimulus.** Occurs when the same surfaces placed on differently colored backgrounds appear to have distinct colors. Taken from [36].

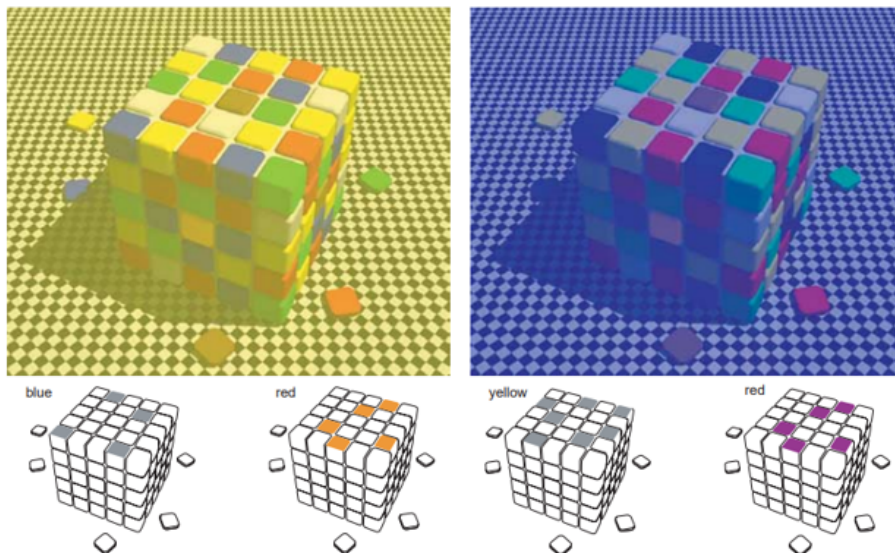


**Figure 1.8: Color contrast and constancy effects produced by empirical generation of visual perceptions.** The upper pictures shows the cubes as if in yellowish (top left) or bluish (top right) illumination. The lower images show specific tiles of interest in the absence of these contexts. Taken from [34].

## 1.2.4 Visual motion perception

Visual perception of motion is essential for human survival. An efficient adaptation to the environment, particularly in interactions with other moving organisms, is made possible by the information that moving objects and self-motion provide. Advancements in neuroimaging, in particular in functional Magnetic Resonance Imaging (fMRI), have brought the potential to study the relation between visual stimuli and human neural activity, improving our knowledge of the processes behind motion perception mechanisms.

The majority of neurons in the visual system have spatially defined receptive fields. As a result, their responses are intrinsically capable of encoding the spatial location of visual inputs and, in principle, can encode the direction of motion through the sequential activation of populations of neurons with different receptive field locations (e.g. acting as a Reichardt detector) [42]. Psychophysical and physiological studies have distinguished between local motion processing, which refers to the sensitivity to the direction of motion in a small region of the visual field, and global motion processing, which represents the sensitivity to the overall direction of motion in extended regions of the visual field [43]. While the processing of local motion depends on direction-selective neurons with smaller receptive fields in the primary visual cortex [44], the perception of global motion is obtained by the integration of different local motion signals [45] mediated by neural networks from extrastriate cortex areas in the dorsal stream [46, 47]. Among these areas are the human Middle Temporal area (hMT) [48], Medial Superior Temporal area (MST) [49], V3A [50], V6 [51] and regions in the IPS [50, 52, 53]. In fact, visual motion processing is supported by a hierarchy of cortical regions that present motion selectivity as early as V1, with potentially some motion dependent signals arising even from the retina [54]. From there, information is relayed downstream to the LGN, which projects mostly to V1 but also with some direct projections to the human Middle Temporal complex (hMT+). V1 also projects directly onto hMT+ which has dense connections with regions around the IPS [55] 1.9.

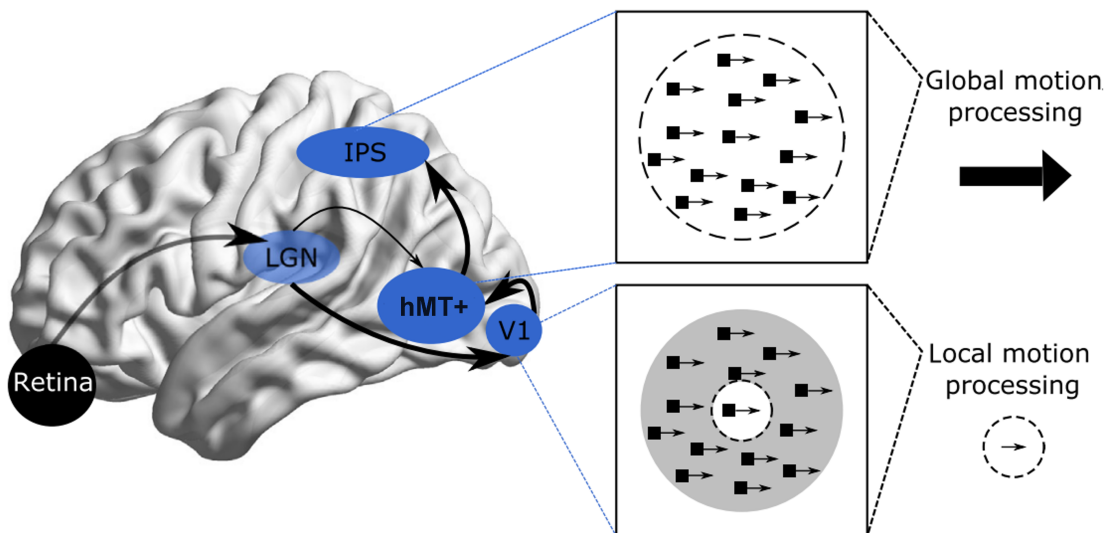


**Figure 1.9: Physical motion processing pathway.** hMT+ represents global motion whereas V1 neurons, which have limited receptive fields, are assumed to reflect local motion. Taken from [55].

The hMT+, located at the junction of the posterior bank of the dorsal limb of

the inferior temporal sulcus with the lateral occipital sulcus [47, 56] (figure 1.10), is considered the central motion selective focus in the human brain and it is composed of hMT and a number of neighbouring regions such as the MST. Activity in hMT+ has been found to be substantially correlated to perception of different types of motion, including apparent motion [57], implied motion [58, 59] and motion aftereffects [60]. Furthermore, comparison between coherent and incoherent motion of light points revealed a major change in activation within the hMT+ that increases linearly with the coherence of motion but shows minor changes in early visual areas [61]. The human brain resolves ambiguity in visual motion in V1 direction-selective cells by including an additional processing step in hMT+, in which pattern motion cells extract the global direction of motion by combining local components [62]. In particular, activation in hMT+ is coincident with perceptual switches during bistable motion of plaid (superimposed gratings with various orientations and motion direction) demonstrating that this region is capable of reliably responding to physical changes in a stimulus' motion characteristics as well as to perceptual changes of a physically constant stimulus [46, 63–65].

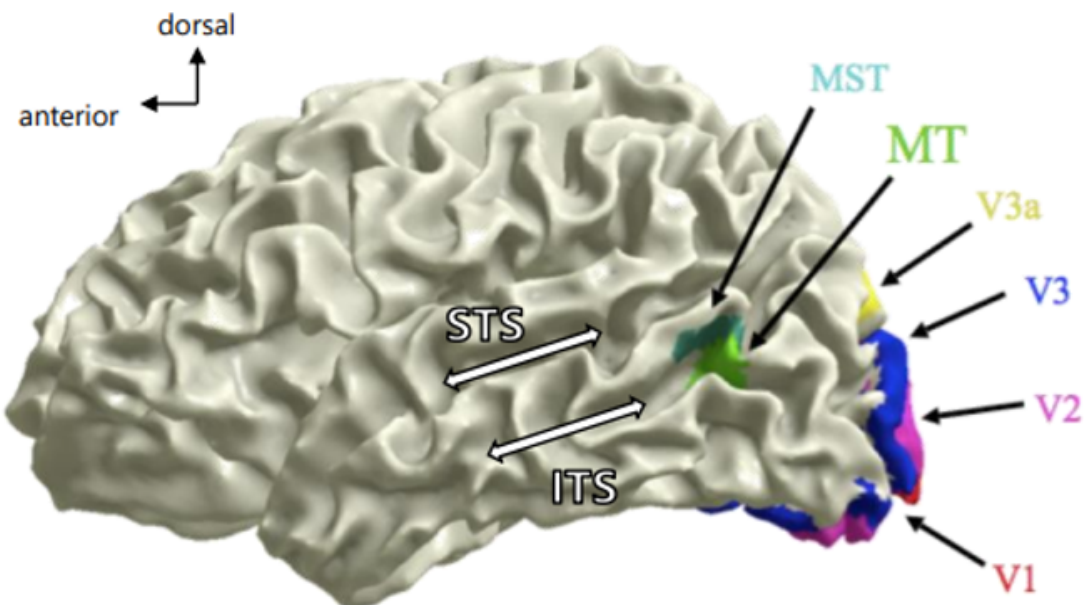


**Figure 1.10: Location of the human Middle Temporal complex (hMT+).** Three dimensional cortical reconstruction of the brain (left hemisphere). Human Middle Temporal area (hMT) (green) falls on the posterior bank of the occipital continuation of the Inferior Temporal Sulcus (ITS), whereas Medial Superior Temporal area (MST) (cyan) falls on the anterior bank. The Superior Temporal Sulcus (STS) is indicated for reference. Other earlier visual areas are shown for reference: V1 (red), V2 (magenta), V3 (blue), V3a (yellow). Adapted from [47].

### 1.2.5 Apparent motion

Apparent motion (AM) is a type of internally generated motion that can be perceived in response to discrete visual stimulation in different positions of the visual field [66]. Under optimal spatial and temporal stimulus conditions, observers can perceive a single stimulus moving continuously along the path between two locations [67] (figure 1.11). In order to respond to apparent motion, neurons must integrate information over a significant portion of visual space, covering at least the distance between the two generating stimuli.

Motion perception in apparent and physical motion are two processes strongly similar, suggesting that, in AM, we actually perceive a stimulus moving along an illusory motion trajectory [68]. In fact, the experience of such AM can be so strong and spatiotemporally specific that it can interfere with the detection of stimuli displayed in the intervening path [69–71]. Similar cortical areas are involved in the perception of apparent and physical motion as several studies have shown the involvement of hMT+ during AM [72, 73]. For example, the application of single-pulse transcranial magnetic stimulation to hMT+ has been reported to reduce the impact of AM on the detection of targets along the illusory motion path [74]. There is also evidence that V1 is critical for AM awareness [75–77], as neurons in this cortical region have been found to respond during AM as if the stimulus was physically present at intermediate locations along the AM path [78], suggesting that AM has an early cortical locus [79]. This activation in V1 may be the result of inhibitory feedback connections from higher visual areas involved in motion, namely the hMT+ [74, 80–82]. In fact, predictive activity related to the visual processing of AM has been reported by several studies [83–85]. According to theories of predictive coding, activation in higher-level visual areas represent the prediction generated by lower-level input, while lower-level responses represent the mismatch between sensory and predicted input. Predictive signals from higher-level regions are sent back to lower-level areas to reduce prediction error by suppressing sensory signals that can be expected based on the higher-level feedback [67]. Several physiological studies have indeed demonstrated that sensory signals, which can be predicted from their surrounding motion context, evoke smaller responses in V1 [30, 86, 87].

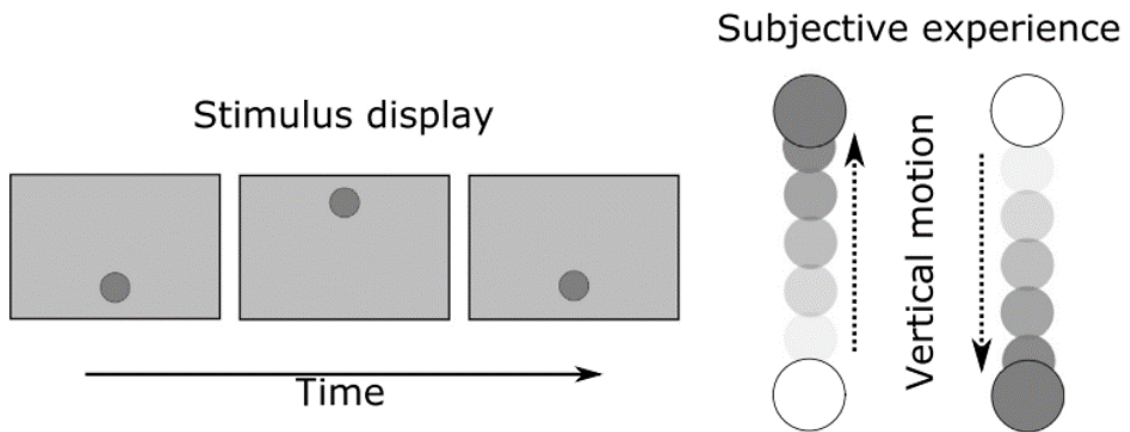


**Figure 1.11: Apparent vertical motion.** When a stimuli is presented quickly over time between different positions, it induces the subjective experience of apparent motion. Adapted from [55].

## 2

# Aims of the project

This chapter aims to explain the background that motivated this thesis, the state of the art of the topic and introduces some concepts necessary to understand it. In the end, the goals of the thesis are presented.

Motion perception arising from sequentially viewing static images has been studied for over 100 years and influenced an entire field of psychology, namely Gestalt theory [88]. Building on this phenomena, since the first description of the Stroboscopic Alternative Motion (SAM) [89], paradigms of ambiguous motion perception have advanced the study of perception, be it in understanding perceptual decision or the underlying working of metastability. However, few studies on this topic have explored the effect of visual stimuli positioning in the visual field, specially regarding meridional differences in motion sensitivity.

Chaudhuri and Glaser [90] used the SAM to provide evidence that the visual system favors motion perception along the vertical meridian, particularly if the fixation point was placed in the center of the stimulus. However, displacing the fixation point along the horizontal meridian significantly reduced this anisotropy, suggesting a reduced correlation of motion signals along the horizontal axis. The study of cognition using metastable and ambiguous paradigms became a prolific field of research, particularly helpful in identifying neural representations of perceptual features [91]. Ambiguous figures also became of interest to study built-in rules and assumptions of the brain when interpreting motion or object identity [92, 93].

The SAM was one figure frequently used in such studies, but the mechanisms behind many of its perceptual features remained unknown, namely: its reliance on relative distance; its dependence on luminance but weaker sensitivity to color or shape cues; and its bias towards intrahemispheric motion upon central viewing. Twenty years after Chaudhuri and Glaser detailed the SAM's vertical bias, Genç et al. [7] was able to show that the microstructure of individually tracked callosal segments connecting motion-sensitive areas of the human Middle Temporal complex (hMT+) can predict the conscious perception of observers. In this manner, the au-

thors were able to confirm, what was previously only hypothesized, that the vertical motion perception bias is due to the fact that, with central fixation, perception of horizontal motion requires integration across hemispheres whereas perception of vertical motion requires only intrahemispheric processing. Additionally, Chiappini et al. [94] went further by manipulating the connectivity between the left and right hMT+ by means of Transcranial Magnetic Stimulation (TMS). They discovered that enhancing the strength of connections from the left to the right hMT+ increased sensitivity to horizontal motion but doing it from the right to the left hMT+ would only result in little perceptual changes. These results reveal that interhemispheric projections between left and right hMT+ are asymmetrical and functionally relevant to horizontal motion perception. Recently, a study focused on the effect of spatial location of the SAM, reported no perception bias across the visual field, neither between upper and lower hemifields nor for motion described as tokens skipping between the two hemispheres [6]. A plausible reason for these conflicting results is that the specific stimulus properties used in this study, such as the Inter Stimulus Interval (ISI), which were substantially different from the previous ones, as well as stimulus size and whether SAM is displayed in short presentations or continuously, caused an impact on perceptual bias [6].

On the other hand, Liu et al. [95] found that a remarkably strong illusion of motion-induced position shift is disrupted at both vertical and horizontal meridians. The authors proposed that motion integration and position processing are affected due to structural features, namely the anatomical gaps of extrastriate areas at both meridians. Specifically, they suggest that neural areas with quadrantic representations in the visual cortex, such as V2 and V3 but not V1, are the initial locus of this motion-induced position shift. A functional consequence of the quadrantic representation of extrastriate areas V2 and V3 had already been proposed by Carlson et al. [96]. In this study, they investigated whether there are quadrant-level effects on attentional selection by using a multiple-target tracking task. The authors observed a stronger interference between targets within the same quadrant than between those separated the vertical and horizontal meridians. This suggests that the interference between attended targets is mediated by areas that maintain a quadrantic topographical representation of the visual field. This findings mirrors crowding effects, whereby the cortical proximity of stimuli can result in interference and loss of acuity [97], showing that anatomical constraints can affect perception.

As detailed above, there have been intriguing discoveries about the influence of the vertical and horizontal meridians as well as their anatomical causes in the perception of motion. However, to the best of our knowledge, no research have

reported a horizontal motion perception bias in the horizontal meridian, contrary to the often reported and fairly understood central vertical bias. Therefore, the objectives of this thesis are the following:

- To study the influence that ambiguous stimulus' positioning has on the perception of apparent motion.
- To provide solid and reliable evidence about the presence of a horizontal motion perception bias when the SAM is positioned on the horizontal meridian of the visual field.
- To understand the visual cortical contingencies that might be behind of the effect mentioned above.

We don't know the rules the brain use, or the limitations it is subject to, when interpreting ambiguous stimuli. For instance, SAM has been know to operate under a policy of shortest path/slowest speed but other contingencies create conditions where the brain might favor a percept that does not adhere to this rule. A topic so broad and malleable as psychophysics can lead to different findings and conclusions because of the multiple factors that can affect it. Hence, we adapted the SAM paradigm to study neuronal competition between sources of long-range apparent motion perception. Using this optimized SAM paradigm, controlling for gaze positioning and performing robust psychometric comparisons, we have arrived at a sensitive measure of a new bias of ambiguous motion perception. We further explored the sensitivity of the identified horizontal bias to stimuli contrast, as an attempt to identify its roots within the early visual cortex processing of ambiguous information.



# 3

## Methods

### 3.1 Participants

Twenty seven participants aged between 20 and 46 took part in the present study - 20 in the first experiment, 7 in the second and 2 in both experiments. Three of them were researchers (participants 01, 02 and 04) and the others were graduate students or researchers from the university of Coimbra, naive to the purpose of the experiment with no experience with psychophysical experiments. All participants had normal or corrected-to-normal vision and had no history of psychiatric or neurological disorders. All participants were able to perceive both configurations of each stimulus and were first accustomed to the stimuli before starting the calibration. Prior to participation all of them gave written informed consent.

### 3.2 Stimulus

In this study, we used a bistable motion paradigm where the perception of apparent motion was induced by the Stroboscopic Alternative Motion (SAM) (figure 3.1.a), commonly studied in vision ambiguity [6, 7, 90]. The SAM consists in flashing two dots simultaneously on diagonally opposite corners of a virtual rectangle (figure 3.1.d - frame 1), which are subsequently switched off and replaced by two dots appearing on the other two corners (figure 3.1.d - frame 2) [7]. When the two frames are presented successively, or within a sufficiently short time, observers can perceive apparent motion, between the dots in separate frames, either along the vertical (figure 3.1.b) or horizontal axis (figure 3.1.c).

Two different types of SAM stimuli were created in MATLAB (The MathWorks, Inc., Natick, MA) using the Psychophysics Toolbox [98]. One was used in the Method of Limits (MoL) and the other was used in the Method of Constant Stimuli (MoCS), both addressed in section 3.3. Visual stimulation for both methods was displayed on a LCD monitor with a refresh rate of 100 Hz and a resolution of

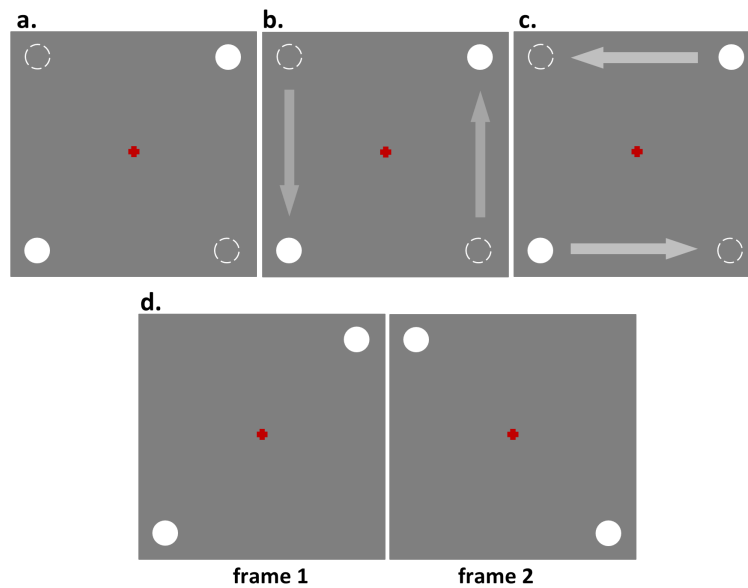


**Figure 3.1: Stroboscopic Ambiguous Motion (SAM) stimulus.** **a.** The SAM is depicted with the first frame in white and the subsequent frame in dashed lines. **b.** Vertical motion perception of the SAM. **c.** Horizontal perception of the SAM. **d.** SAM's frames 1 and 2. When alternating between these two frames, apparent motion can be perceived in both axes.

1440 x 1080 pixels at a distance of 88 cm from the participant. The participant's head position was fixed with a chin rest. The laboratory was in a low-illumination environment.

Regarding the MoL stimulus, each set of two dots was displayed for 183 msec with an Inter Stimulus Interval (ISI) of 67 msec during which no dots were shown. For the MoCS stimulus each frame was shown for 220 msec with an ISI of 30 msec. In both cases, a cycle was completed when two frames of dots were presented (see figure 3.1.d), including two ISI in both stimuli, meaning each cycle had a duration of 500 msec. Therefore, 2 full cycles were displayed during 1 second meaning a stimulus frequency of 2 Hz for both stimuli. In the first experiment, all stimuli dots (diameter,  $0.3^\circ$  of visual angle; luminance,  $153 \text{ cd/m}^2$ ) were presented on a gray background (luminance,  $79 \text{ cd/m}^2$ ) displaying a virtual rectangle of  $1.5^\circ \times 1.5^\circ$  (visual degrees), when the horizontal and vertical distance between the dots is the same. In the second experiment, all stimuli dots had the same diameter but variable luminance (as explained in the next chapter), and were displayed on a darker background (luminance,  $7 \text{ cd/m}^2$ ) within the corners of a virtual rectangle with the same dimensions as in experiment 1. All stimuli virtual center were placed at 3 visual degrees from a red fixation cross (diameter,  $0.1^\circ$  of visual angle) displayed at the center of the screen. We used luminance measurements already available in

the laboratory. These measurements were obtained with the PR-650 SpectraScan Colorimeter from Photo Research, Inc from 18 grey levels. A gamma function was fit to the luminance measurements obtained and used to estimate the luminance of the stimuli used in our study.

### 3.3 Ambiguous Stimuli Calibration - Procedure

In this section we explain all the methods and conditions used in the calibration process of individual psychometric parameters used in this study.

#### 3.3.1 Determining individual Parity Ratios

As said before, the SAM is an ambiguous stimulus of apparent motion that leads to perceptions of either horizontal or vertical motion [7]. When the horizontal and vertical distances between the dots is the same, i.e an aspect ratio (horizontal distance divided by vertical distance) of 1, perception should ideally be equiprobable. However, this is not true as there is significant difference in the tendency to see vertical or horizontal motion between distinct subjects [7]. This is manifest mostly for stimuli displayed in the central vision but might also be found in the current setting. Therefore, in order to study the perception bias along the horizontal meridian it was beneficial to create a stimulation paradigm that could be easily biased toward either of two possible perceptions with just minor changes to the stimulus' basic parameters. In fact, a simple adjustment to the SAM's aspect ratio can easily bias perception towards horizontal or vertical perception [90]. For this reason, an initial estimate of the parity ratio for each participant had to be determined in order to ensure that the stimulus was appropriately biased to influence the observer in favor of one percept more frequently than the alternative, i.e. having a dominance of one percept over the other [1]. The parity ratio is the optimal aspect ratio that leads to equal durations of horizontal and vertical motion perceptions [7]. In other words, it is the ratio between horizontal and vertical distance for which the participant has a 50% probability of perceiving both vertical and horizontal motion. This measure is intrinsic and can vary widely between participants. [7, 99]. To be able to quantify participant's Parity Ratio (PR) when viewing the SAM, we adopted a procedure previously used by Genç et al. (2011) and Kohler et al. (2008), that uses a combination of two standard methods in psychophysics: the Method of Limits and the Method of Constant Stimuli.

### 3.3.1.1 Method of Limits (MoL)

The MoL is one of the most used psychophysical tools. This approach involves changing a stimulus parameter, such as contrast, brightness or, in this study's case, aspect ratio, from trial to trial until the observer reports a shift in perception. MoL is performed in two phases, the ascending phase and the descending phase, with the stimulus' parameter being varied in opposite ways [1]. In the ascending phase, the value to be changed starts at a low level forcing a specific perception in the participant (e.g. can see the stimulus or not; can only perceive horizontal or vertical motion). This value is gradually increased until it reaches a threshold where the participant's perception inevitably changes (e.g. stimulus became visible ; stimulus apparent motion "switched" from vertical to horizontal). Likewise, during the descending phase, that same parameter begins with a high value where one perception is ensured and steadily decreases until the observers perception shifts. (e.g. participant stops seeing the stimulus; participant starts seeing vertical motion rather than horizontal motion) [100]. The average of all switch points values, i.e. the points where there was a change in perception, in the ascending and descending trials, is used to estimate the absolute threshold which, in this research, corresponds to the PR (figure 3.2). Ascending and descending series often yield slight but systematic differences in switch points. Therefore, the two types of series are usually used in alternation [101].

Stimulus Intensity	Alternating Ascending and Descending Series					
	1	2	3	4	5	6
0	N		N		N	
1	N		N		N	
2	N		N	N	N	
3	N	N	N	Y	N	N
4	N	Y	N	Y	N	Y
5	N	Y	Y	Y	Y	Y
6	Y	Y		Y		Y
7		Y		Y		Y
Transition Points	5.5	3.5	4.5	2.5	4.5	3.5

Threshold = Average Transition Points =  $(5.5+3.5+4.5+2.5+4.5+3.5)/6 = 24/6 = 4$

**Figure 3.2: Method of Limits (MoL).** Determination of Absolute Threshold. Response (Stimulus Perceived): yes (Y), no (N). Adapted from [101].

Despite being simple to use, the MoL is susceptible to two different types of errors: the habituation error and the anticipation error. In the first, the observer may not report a change in perception beyond the threshold in the descending or ascending phases. In the second one, the participant may anticipate by reporting a change in perception before the threshold in either the descending or ascending series leading to an overestimated threshold detection [100] [1].

### 3.3.1.2 Method of Constant Stimuli (MoCS)

The MoCS evaluates the participant's response to a fixed set of stimuli across a range of stimulus values made so that encompasses the absolute threshold value obtained with a previous exploration (e.g. using the MoL). This preselected set of stimuli is repeatedly shown in a random order, ensuring that each will occur with equal frequency and that no effect will systematically be carried over from one condition to the next. After each trial, the observer reports his perception of the stimulus (e.g. detected or not detected; vertical motion or horizontal motion). Once each stimulus value has been presented multiple times, the proportion of responses is calculated for each stimulus level (table 3.1). The data are then plotted in a graph of probability of detection versus stimulus values which is also called psychometric function (figure 3.3) [100][101].

**Table 3.1: Method of Constant Stimuli (MoCS) data.** The percentage of perceived stimuli is given by the quotient of the frequency of perceived stimuli and the number of trials for each stimulus intensity. In this example, each stimulus intensity is presented in 50 trials. From [101].

<b>Stimulus Intensity (arbitrary units)</b>	1	2	3	4	5	6	7
<b>Frequency of Perceived Stimuli</b>	1	3	12	20	37	45	50
<b>Percentage of Perceived Stimuli</b>	2	6	24	40	74	90	100

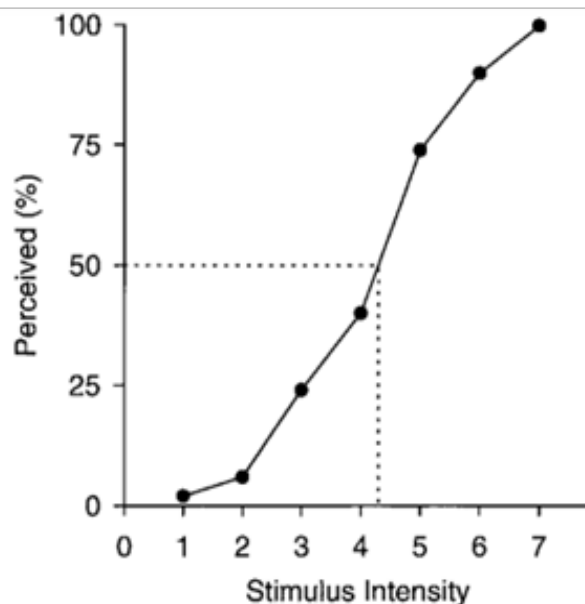


**Figure 3.3: Psychometric Function.** The percentage of times a stimulus is perceived and the related stimulus intensity are shown by a psychometric function. The threshold is defined as the intensity at which the stimulus is detected 50 percent of the time. Adapted from [101].

If there was a fixed detection threshold, the psychometric function should show an abrupt change from "not perceived" to "perceived". However, psychometric functions seldom conform to this all-or-none rule [101]. What is typically obtained is a sigmoid curve, which shows that lower stimulus intensities are occasionally detected and higher values are more frequently detected, with intermediate values being occasionally detected but not always. The S-shaped curve of the psychometric function results from different sources of variability being one of them the continual fluctuations in sensitivity inherent to biological sensory systems [101].

In any case, the intensity value of the threshold must be determined statistically since it happens with a specific probability. Conventionally, the absolute threshold measured with the MoCS is given by the intensity value that elicits a particular response or perception in 50% of the trials [101]. Estimation of this threshold almost always requires interpolation from the data obtained.

Albeit the approach of continual stimulation is assumed to offer the most accurate threshold estimations, its major drawback is that it is relatively time-consuming and demands a patient, attentive observer due to the numerous trials needed [101]. Moreover, effects of adaptation start influencing perception over longer presentations and for the purposes of the current study would add unnecessary noise.

### 3.3.2 Visual Tasks

Two experiments were designed for this study to assess different aspects of participant's perception. In each one of them, the observers had to perform the MoL and MoCS tasks with different conditions.

In the case of the MoL task, it was the same for both experiments except for its background luminance (79 cd/m<sup>2</sup> for experiment one and 7 cd/m<sup>2</sup> for the experiment two). The visual stimuli were a set of 40 trials, 20 for the descending phase and 20 for the ascending phase in random order, placed in the horizontal meridian.

In ascending phases, the stimulus aspect ratio started at 1/3 (figure 3.4.A) making it so that the participant first perceived horizontal apparent motion, since the horizontal distance between the dots was three times less than the vertical distance. Throughout the trial, the aspect ratio was gradually increased until either the observer reported a perceptual change from horizontal to vertical perception, by key pressing, or it reached the ratio of 3 (figure 3.4.B), ending the current trial and randomly starting a new ascending or descending trial. Inversely, in descending phases, the aspect ratio started at 3 inducing the participant to perceive vertical apparent

motion (horizontal distance was three times bigger than the vertical distance) and it was gradually decreased until the participant started to perceive horizontal motion or it reached the value of  $1/3$ . Between trials, a "Ready..." message was displayed for 1.5 seconds so the participant could prepare for the next one. When the aspect ratio was equal to 1 the stimulus horizontal and vertical dimensions were  $1.5^\circ$  each, in visual angles. As mentioned in earlier sections, the mean value of the switch points ratio obtained for both ascending and descending conditions was used to calculate the initial PR estimate.

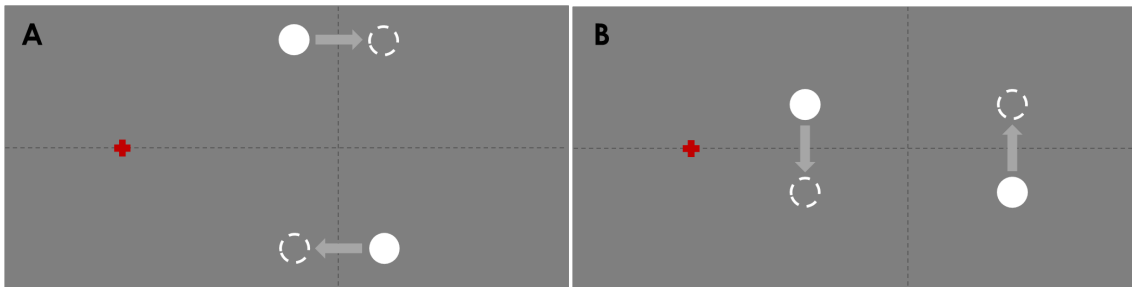


**Figure 3.4: Stroboscopic Alternative Motion (SAM) phases used in the Method of Limits (MoL).** **A)** First frame of the ascending phase – the SAM begins with an aspect ratio of  $1/3$  which is gradually increased. **B)** First frame of the descending phase – the SAM starts with an aspect ratio of 3 which is gradually decreased. Arrows indicate the direction of the perceived motion. The red cross is located at the center of the visual field and participants are instructed to fixate it throughout the task.

When compared to previous studies that used MoL [7] [99], some modifications were made in the present experimental designs. In those studies, the horizontal length was kept constant while the vertical distance was ramped up during the ascending series and down during the descending ones. As expected, this procedure has the impact of favoring perception of vertical or horizontal motion. However, it results in a change in the scale of the stimulus since its area will change depending on whether one of its dimensions is increased or decreased. Moreover, a similar strategy with a ratio of  $1/3$  or 3 might result in a stimulus where the dots fall near the edges of the participant's peripheral vision. Therefore, it was chosen to keep the stimulus imaginary rectangle's area constant in order to keep it centered and avoid engaging visual field areas that would be too disparate for equivalent stimuli. Thus, in each incremental step of the ascending and descending phases, both vertical and horizontal dimensions were inversely changed. Hence, if the height of the stimulus increased then its width decreased and vice-versa [1].

Regardless of the trial being ascendant or descendent, the incremental steps

that increased or decreased the stimulus aspect ratio were given by:

$$I_{step} = \frac{\log_{10}(R_{max}) - \log_{10}(R_{min})}{n}$$

Where  $R_{max}$  and  $R_{min}$  are the initial ratios for the descending and ascending series, respectively, and  $n$  is the number of steps, which was set to 60.

The reason for using the logarithm in incremental step calculations is straightforward and is best illustrated by the following example taken from [1]. A rectangle with a width of 3 and a height of 9 corresponds to a stimulus with an aspect ratio of 1/3, which is in one end of the MoL's ratios range for this research. In the opposite end, the stimulus must have a width of 9 and a height of 3, corresponding to a ratio of 3. Comparing the values, it is possible to notice that, starting at a ratio of 1 (i.e. the dots' positions fall on the vertices of a square), it takes 6 increments of 1/3 to reach the ratio of 3 while a reduction of only 2 steps to get from 1 to the ratio of 1/3. However, if the ratio's value is converted to logarithm, it is possible to subtract and add the same value which results in an equal increase and decrease of the aspect ratio. This way, it is possible to produce a range of stimuli throughout the series that are symmetrical around the ratio of 1. Taking the same previous example, the logarithm of the ratio 1/3 is equal to -0.4771 and the logarithm of the ratio 3 corresponds to the value 0.4771. Both are 0.4771 apart from logarithm of 1 which is 0. Knowing this, a logarithmic scale was used to calculate the incremental steps as it is shown above.

As it was said before, two different MoCS tasks were created for the next part of the study. In experiment 1, participants viewed the SAM with eight subject-dependent aspect ratios in 4 different positions per hemisphere (figure 3.5). The 90° and 270° positions functioned as control ones. They were used to confirm the already known vertical bias existing when the stimulus was displayed on the vertical meridian [7]. One of the eight aspect ratios was the PR initial estimate obtained in the MoL task while the remaining seven were placed around the first, with four being bigger and three being smaller than the original PR. Every point was apart 0.08 to the ratio's logarithm of the previous one. The linear values for the 8 ratios were obtained by simply applying the exponentiation. In this part of the visual task, participants were shown 4 trials per ratio per position, presented randomly in each run. Due to the high number of trials (8x4x4), in order to avoid habituation to the task, all trials were presented with a random Inter Trial Interval (ITI) of 1 to 1.5 seconds of duration. The stimulus was displayed for 1.5 seconds (3 full cycles). At the end of each trial, participants were required to record, by button press, whether



they perceived motion in the horizontal or vertical axis. Every response period had a duration of 1 second during which the fixation cross turned blue. Each participant had to complete 5 runs per hemisphere, of 8 minutes and 20 seconds each. Each hemisphere was tested in different days with two to three weeks apart, except for participant 07 which, for personal reasons, was not able to perform the task for the right hemisphere. Half of the participants started the tests with the right hemisphere and the other half with the left hemisphere. Before beginning the assignment, all participants were given the task instructions and were familiarized with the stimuli.

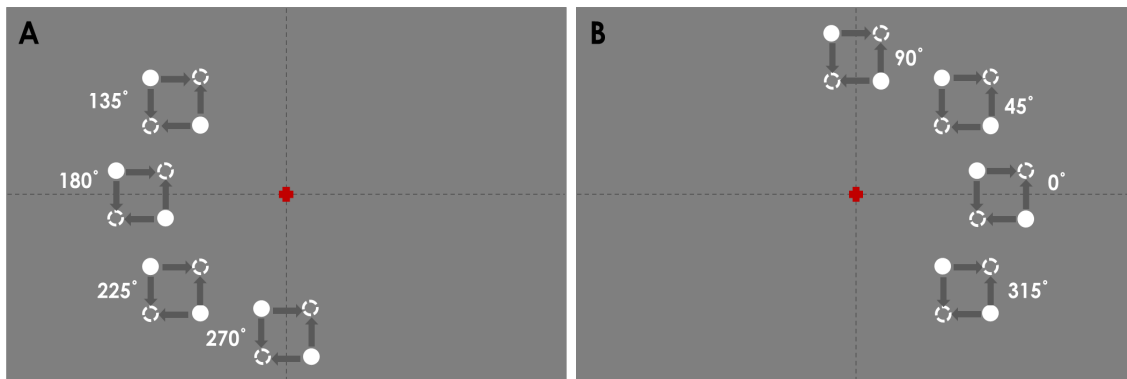


**Figure 3.5: Stroboscopic Alternative Motion (SAM) positions used in the Method of Constant Stimuli (MoCS).** The left hemifield positions were 135°, 180°, 225° and 270° (A) and right hemifield positions were 0°, 45°, 90° and 315° (B), considering the trigonometric circle. The positions 0° and 180° correspond to the horizontal midline of the right and left hemifields, respectively. The 90° and 270° positions functioned as control positions. Arrows indicate the direction of the perceived motion. The red cross is located at the center of the visual field.

In experiment 2, the set of stimuli with eight subject-dependent aspect ratios was built in the same way as in experiment 1. However, these stimuli were not distributed over four positions, instead they were seen with 5 different luminances in the same positions of the horizontal meridian (0° and 180°). The luminance was assigned for each stimulus as a measure of the Michelson Contrast (MC):

$$MC = \frac{L_{stim} - L_{backg}}{L_{stim} + L_{backg}} \Leftrightarrow$$

$$L_{stim} = \frac{-L_{backg}(1 + MC)}{MC - 1}$$

Where MC is the Michelson contrast,  $L_{stim}$  is the stimulus' luminance and  $L_{backg}$  is the background's luminance.

Five different MCs (5%, 10%, 20%, 40% e 80%) were used in this experiment. Similar to experiment 1, all additional stimuli sets and conditions were used. Ob-

servers were presented with 4 trials per ratio per contrast (160 trials total). Each participant had to complete 5 runs of 8 minutes and 20 seconds each, in only one hemisphere. Half of participants for this experiment did the task in the right hemisphere while the other half did it in the left hemisphere. In both experiments, the data obtained was then used to plot the psychometric functions (section 3.4). In all tasks participants were monitored using an eyetracking system to monitor gaze fixation but due to technical issues only 19 out of the 27 participants had usable recordings (see section 3.5).

### 3.4 Psychometric Function fitting

Psychometric functions relate the participant’s behavior on a specific psychophysical task to some physical stimulus characteristic (e.g. contrast, aspect ratio). This type of function is typically measured in order to identify one or more parameters that influences the participant’s behavior, as a threshold contrast for visual detection or a point of subjective equality for perceptual decision (e.g. parity ratio) [102].

In this thesis, the psychometric functions were fit using the Palamedes toolbox, which is a set of routines and demonstration programs written in MATLAB for analyzing psychophysical data. [102]

There are 5 key components to measuring and fitting a psychometric function that translate to this project in the following way:

- **Choosing the stimulus levels:** the 8 subject-dependent values of aspect ratio.
- **Selecting the function to fit the data:** we used the logistic function [7] as it provides a good fitting to visual task’s data [102]. This function is given as:

$$F_L(x; \alpha, \beta) = \frac{1}{1 + \exp(-\beta(x - \alpha))}$$

Where  $\alpha$  defines the overall position of the curve along the abscissa and, for logistic functions, corresponds to the aspect ratio at which the vertical motion perception is at 0.5 or 50%, i.e., the PR. The parameter  $\beta$  determines the slope or gradient of the curve. These factors represent properties of the underlying sensory mechanism and are called free parameters because they are allowed to vary during fitting.

However, there are two other parameters,  $\gamma$  and  $\lambda$ , necessary to fully characterize the psychometric function. The parameter  $\gamma$  is the guessing rate and describes chance-level performance. In other words, it is the proportion of

correct answers that can result from simple guessing. In this work's experiments there are no correct or incorrect answers, therefore a value of zero was attributed to parameter  $\gamma$ . The parameter  $\lambda$  is known as the lapse rate and corresponds to the probability of responding incorrectly as a result of a lapse. For the purposes of the current study this factor was also considered zero meaning minimum and maximum probabilities were fixed at 0 and 1. Lapsed responses would correspond to missing a key press, in other experiments this could lead to a ceiling below 1 or bottom above 0 for the logistic fit, as there would be trials with no response. In the current setting this was not the case since only the trials with a participant's response were considered for estimating the perceptual dominance. Both  $\gamma$  and  $\lambda$  parameters are considered fixed parameters as they are not allowed to vary during the fitting [102][1].

- **Fitting the function:** to fit the logistic curve to the data, the Palamedes iteratively went through a range of potential values for the  $\alpha$  and  $\beta$  parameters. However, the precise value of the observer-specific parameters  $\alpha$  and  $\beta$  is unknown. The fitting process instead looks for estimates of these values that led to a curve that most closely matched the experimental data. The method used for fitting the psychometric function was the maximum likelihood criterion, which defines the best-fitting psychometric function as the one most likely to reproduce the experiment as it was carried out by the human observer [102][1].
- **Estimating the errors on the function's parameter estimates:** the Standard Error (SE) of the threshold and the SE of the slope are estimates of the errors related to the estimations of  $\alpha$  and  $\beta$ . In other words, they are measures of how far the estimates are likely to be from the true value of  $\alpha$  and  $\beta$ . The SEs are calculated using a technique known as bootstrap analysis, which randomly creates several hypothetical sets of data, 400 in this work's case, from the real experimental data. The logistic function is then fitted to each new hypothetical data set in order to estimate  $\alpha$  and  $\beta$ . The standard deviations of these values across all the sets are then calculated and represent the final estimate of the errors on the parameters [102][1].
- **Determining the goodness-of-fit of the function:** in general, it would be indicative of a good fit if the data points fell exactly along the fitted psychometric function, whereas if the data points fell some distance from the function it would be suggestive of a bad fit. The goodness-of-fit function in the Palamedes toolbox uses the method described in Wichmann and Hill (2001) [103]. Briefly, a Monte Carlo distribution is produced with a defined

number of synthetic datasets and with the original data, produced by randomization, from which deviance parameters are obtained. An associated p-value corresponding to the proportion of simulations with greater deviance than the original data are used to determine whether the fitted function provides an adequate model of the data. The p-value has a range between 0 and 1, and the larger it is the better the fit. Conventionally, researchers agree that the fit is unacceptably poor if the p-value is less than 0.05 [102][1].

## 3.5 Eye tracking

An infrared eye-tracking system was used in order to record the participant's eye movement data as a control measurement for the influence of gaze positions. This procedure was crucial to this work since it allowed to verify if the participant fixated the red cross during the stimulus presentation. Consequently, this assures that the SAM was displayed consistently over the same retinal position and that the results obtained were not influenced by changes in the stimulated visual field or eccentricity.

### 3.5.1 Procedure

The EyeLink 1000 Plus (SR Research Ltd., Canada) eye tracker was used in 19 of 27 participants. The system was assembled according to figure 3.6. At the beginning of each block of trials, the eye tracker was calibrated and validated by mapping the correspondence between 9 target locations and the gaze position when volunteers viewed each location, with their heads fixed by a chin rest. Calibration and/or validation were repeated until the validation error was smaller than 1 degree of visual angle for all targets. The gaze position error, the difference between the target position and the computed gaze position, was on average  $0.617^\circ$ . Afterwards the volunteers would initiate the tasks described before. In these conditions, this eye tracking system has a accuracy down to  $0.15^\circ$  ( $0.25^\circ - 0.50^\circ$  typical) and a spatial resolution of  $0.01^\circ$  of visual angle. During the experiments, the EyeLink 1000 Plus recorded the participant's gaze position (x and y coordinates) at a sampling rate of 1000 Hz and a illumination power of 75 to 100% adjusted for each subject in order to achieve a stable threshold of pupil and corneal reflection setting. Only the gaze position of the participant's dominant eye (right or left) was recorded. Despite solely tracking one eye, participant's viewing of the stimuli was binocular. The eye tracker software also received triggers from the stimulus PC indicating the onset of responses by button press. The EyeLink control system was programmed in Matlab

(The MathWorks, Inc., Natick, MA) using the corresponding EyeLink toolbox [104]. Fixation density plots were made to better visualize the data obtained.

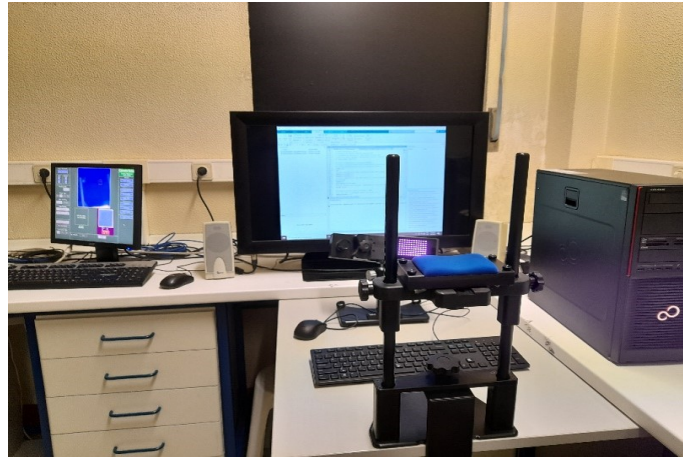


**Figure 3.6: Infrared oculographic eye tracker.** Eyetracking system used for participant's gaze position measurement.

### 3.5.2 Data Processing

The gaze position data coming from the eye tracker was centered by subtracting half of the screen's resolution. In other words, the horizontal data ( $x$  axis) was subtracted by  $1440/2$  and the vertical data ( $y$  axis) was subtracted by  $1080/2$ , so that the screen's center would be in the coordinates  $(0,0)$ .

As indicated before, every trial had a duration of 3.5 to 4 seconds. However, the only period where it is crucial to verify the participant's gaze position is the stimulus presentation period which lasts for 1.5 seconds. Therefore, the data corresponding to 1 second before the beginning of every trial was eliminated as well as the data corresponding to the response time (1 second after the stimulus presentation).

In order to choose what trials needed to be excluded due to eye movements away from the fixation target and, therefore, not used in the psychometric functions, a "window" was created to represent where the participant's gaze could be positioned successfully. This window's dimensions are given by the interception between the stimulus imaginary square with the lowest aspect ratio and the stimulus imaginary square with the highest aspect ratio, on average for all participants. That being the case, the width ( $x$  axis) of this window is 47,5 pixels ( $1,13^\circ$  of visual angle) and its height ( $y$  axis) is 43,8 pixels ( $1,04^\circ$  of visual angle). Henceforth, a window with twice this dimensions was used in the criteria. Therefore, a trial would be included or not accordingly to the following criteria:

- When, for any reason (blinks, eye tracker malfunctions), more than half of a trial does not present ocular position data in any axis, the trial would be removed from the data and not used in both the psychometric functions fitting and fixation density plots.
- When less than 90% of the trial's horizontal or vertical data is within the limits of the calculated window, the trial would not be used in the psychometric functions fitting despite being used in the fixation density plots.

After the removal of the excluded trials, the fixation density plots were built in Matlab (The MathWorks, Inc., Natick, MA). Each completed run had an associated plot. The average time spent inside the defined limits was estimated for each participant as was the trial mean horizontal and vertical gaze position which were used to normalize the fixation density plots. On average, the average time spent inside the limits was 94.5%. In experiment 1, usable eye tracking data for 14 of the 18 participants was obtained and for 1 participant in the second experiment. Issues with obtaining eye tracking data were mainly the inability to get reliable data from a few participants wearing glasses, in experiment 1, and due to an error in the autosave of files, in experiment 2.

### **3.6 Statistical Analysis**

For the statistical analysis, GraphPad Prism 8 (GraphPad Software Inc., CA, USA) was used. Statistical significance resulting from two independent variables, e.g. main-effect hemisphere and main-effect stimuli position, was determined by a two-way analysis of variance (ANOVA). A one-way ANOVA was used for comparisons with only one independent variable. Significantly different means were identified using the Tukey's multiple comparisons test. An alpha level of 0.05 was used for all statistical tests.

# Results and Discussion

This chapter presents the results of the previously described tasks and its respective discussion. It starts with the results of the preliminary tests followed by the first and second experiments' results. The main results correspond to the psychometric fits and the control analysis for strict gaze position control.

## 4.1 Preliminary Work

This section presents preliminary work concerning the proposed approach to study perceptual decision of ambiguous motion. This first test can be interpreted as a proof-of-concept and also provided preliminary evidence of the phenomena to be further studied. In order to evaluate the influence that stimulus position has in how one perceives motion, 7 participants (aged between 20 and 48 years old) took part in a Stroboscopic Alternative Motion (SAM) test created in MATLAB (The MathWorks, Inc., Natick, MA). The SAM configuration was, in all aspects, similar to the one used in the rest of the thesis except for the distance between the center of the virtual square and the center of the screen which, in this case, was 2 visual degrees instead of 3. All stimuli had an aspect ratio of 0.8 and were displayed during 700 ms, in 9 different positions, the 8 used in the Method of Constant Stimuli (MoCS) task (see figure 3.5) and one more at the center of the screen. Both hemifields were tested in the same run. All participants completed 3 runs (90 trials each). At the end of each trial, participants had to report their perception of apparent motion by button press as described in section 3.3.2. The results were grouped by stimulus position and are summarized in figure 4.1. As expected the vertical meridian positions as well as the centre position exhibit a vertical motion perception bias related to the facilitated intrahemispheric processing of visual data [7]. In order to test whether the stimulus positioning along the visual field could influence the participant's perception, a one-way repeated measures analysis of variance (ANOVA) was conducted. A significant effect of the stimulus position was found ( $F(2,12)=20.86$ ,  $p=0.0001$ ). Post hoc analyses using the Tukey's multiple comparisons test indicated

that the average perceived vertical motion was significantly lower in the horizontal meridian positions ( $25.067 \pm 7.616$ ; mean  $\pm$  *Standard Error of the Mean (SEM)*) when compared to both vertical meridian positions ( $78.242 \pm 6.106$ ; Tukey's post-hoc test,  $p=0.0054$ ) and centre position ( $66.786 \pm 8.350$ ; Tukey's post-hoc test,  $p<0.0001$ ), as one would expect [7]. Furthermore, the perceived vertical motion was marginally lower in the horizontal meridian positions than in both top ( $38.421 \pm 9.403$ ; Tukey's post-hoc test,  $p=0.0995$ ) and bottom ( $42.265 \pm 7.921$ ; Tukey's post-hoc test,  $p=0.0734$ ) positions. The fact that top and bottom positions show fairly similar vertical perception and that horizontal meridian shows a tendency towards less frequent vertical perception suggests that: 1) there might be a difference in perception between these positions; and 2) this difference is not explained by the same factors of the vertical perception bias in the vertical meridian (i.e. intrahemispheric bias). Two main factors may have contributed for this difference being only tentative and not immediately significant:

- All stimuli had an aspect ratio of 0.8 and thus differences could only be inferred from small deviations in this single condition and relative from one position to the other. Moreover, since there was no calibration of the participant's parity ratio, the conditions tested might have been not ideal for each subject. One can see this as a participant with a Parity Ratio (PR) below 0.8 will have a tendency to perceive more vertical apparent motion considering that the stimulus aspect ratio is above the point of equal motion perception (see figure 3.3). In the same way, if the participant's PR is above 0.8, the participant will perceive horizontal apparent motion in most trials. This results in increased noise due to intersubject variability and a less robust estimate of perceptual differences for each position.
- These pilot tests were carried out during the COVID-19 pandemic and thus an effort was made to perform the task under social distancing conditions. Hence, all tests were performed remotely and it was not possible to guarantee equal conditions for each participant as the experiments took place at home. Nonetheless, stimuli parameters and protocol guidelines were followed as closely as possible.

Therefore, it made sense to further explore the stimulus position influence in the visual stimulus perception in a more controlled study, with more sensitive methods, and taking place in a laboratory that can provide the optimal environment to conduct longer experiments with more volunteers.



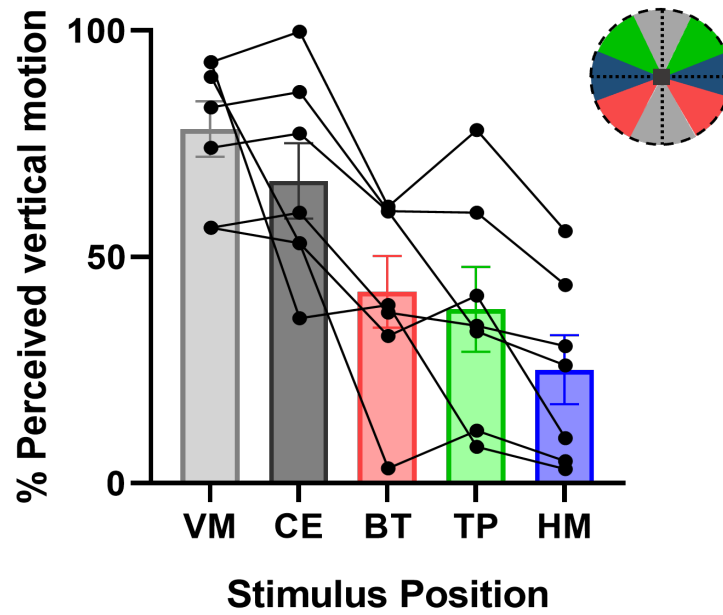


**Figure 4.1: Percentage of vertical motion perception for all participants per stimulus position.** Stimulus positions were organized in five different groups: Vertical Meridian positions (VM) -  $90^\circ$  and  $270^\circ$ ; Central position (CE); Bottom positions (BT) -  $225^\circ$  and  $315^\circ$ ; Top positions (TP) -  $45^\circ$  and  $135^\circ$ ; Horizontal Meridian positions (HM) -  $0^\circ$  and  $180^\circ$ . Bars depict mean  $\pm$  SEM. Circles depict individual values from each participant.

## 4.2 Visual Tasks

In this section we show the results and discussion of the visual tasks for experiments 1 and 2.

### 4.2.1 Experiment 1

As explained before, the MoCS task was carried out using a set of eight vertical motion percept proportions (ratio between the number of trials vertically perceived and the total number of trials), one value for each aspect ratio and a set for each one of the eight positions tested (see figure 3.5). The ratios were selected based on approximate estimates of PR (see section 3.3) in order to achieve an optimal sampling for each subject. The 4th ratio corresponds to the first estimate of the PR obtained using the Method of Limits (MoL). Table 4.1 and 4.2 show the results obtained from MoCS task for the left and right hemifields, respectively, for participants 03, 06 and 14 as well as the average for all participants.

From the data presented in the tables, the vertical bias expected in the control

**Table 4.1: Percentage of vertical motion perception of participants 03, 06, 14 as well as the average for all participants, for each position used in the visual stimulus of the left hemifield.**

Participant	Position	1 <sup>o</sup> Ratio	2 <sup>o</sup> Ratio	3 <sup>o</sup> Ratio	4 <sup>o</sup> Ratio	5 <sup>o</sup> Ratio	6 <sup>o</sup> Ratio	7 <sup>o</sup> Ratio	8 <sup>o</sup> Ratio
03	180°	0	0	0	26.3	65.0	1	100	100
	135°	5.0	0	0	40.0	83.3	100	100	100
	225°	0	52.6	65.0	94.7	100	100	100	100
	270°	20.0	75.0	95.0	100	100	100	100	100
06	180°	0	0	0	10.0	22.2	75.0	100	100
	135°	0	5.0	0	10.0	40.0	80.0	95.0	100
	225°	0	0	5.3	40.0	85.0	100	100	100
	270°	75.0	85.0	90.0	100	95.0	100	100	100
14	180°	0	0	0	25.0	42.1	89.5	94.7	100
	135°	0	0	0	50.0	93.3	100	100	100
	225°	0	0	27.8	40.0	82.3	100	100	100
	270°	95.0	100	100	100	100	95.0	100	100
Mean ± SEM	180°	5.9 ± 2.3	9.0 ± 2.9	17.3 ± 4.0	35.6 ± 5.3	58.1 ± 4.6	84.6 ± 3.0	94.3 ± 1.9	97.7 ± 1.1
	135°	7.1 ± 2.7	15.9 ± 4.8	30.6 ± 5.8	55.3 ± 5.3	79.4 ± 4.4	93.4 ± 2.0	97.3 ± 0.9	98.9 ± 0.6
	225°	10.1 ± 3.3	23.9 ± 5.0	45.1 ± 6.4	68.8 ± 6.1	85.3 ± 3.6	95.5 ± 3.2	98.3 ± 1.7	98.7 ± 0.8
	270°	57.6 ± 7.4	78.9 ± 5.6	87.6 ± 3.4	94.8 ± 1.7	98.2 ± 0.7	99.2 ± 0.6	99.7 ± 0.3	100 ± 0

**Table 4.2: Percentage of vertical motion perception for participants 03, 06, 14 as well as the average for all participants, for each position used in the visual stimulus of the right hemifield.**

Participant	Position	1 <sup>o</sup> Ratio	2 <sup>o</sup> Ratio	3 <sup>o</sup> Ratio	4 <sup>o</sup> Ratio	5 <sup>o</sup> Ratio	6 <sup>o</sup> Ratio	7 <sup>o</sup> Ratio	8 <sup>o</sup> Ratio
03	0°	0	0	0	25.0	70.0	100	100	100
	45°	5.0	0	21.1	50.0	100	100	100	100
	315°	0	0	5.0	73.3	94.4	100	100	100
	90°	25.0	57.9	89.5	95.0	100	100	100	100
06	0°	0	0	15.0	35.0	65.0	90.0	100	100
	45°	0	0	5.0	52.6	89.5	95.0	100	100
	315°	5.0	20.0	50.0	94.7	100	100	100	100
	90°	40.0	78.9	100	100	100	100	100	100
14	0°	0	0	0	5.0	20.0	85.0	94.7	100
	45°	0	0	17.7	43.8	75.0	100	100	100
	315°	0	5.3	22.2	77.8	94.7	100	100	100
	90°	89.5	100	100	94.7	100	100	100	100
Mean ± SEM	0°	4.6 ± 2.0	6.3 ± 2.3	15.3 ± 3.7	36.5 ± 4.8	59.2 ± 4.2	84.3 ± 2.8	93.9 ± 2.3	99.0 ± 0.8
	45°	3.8 ± 1.0	11.1 ± 3.2	28.0 ± 4.6	53.3 ± 4.8	79.5 ± 4.4	91.6 ± 1.8	98.5 ± 0.8	99.5 ± 0.5
	315°	10.9 ± 3.3	22.5 ± 5.0	41.8 ± 6.0	76.4 ± 3.5	91.3 ± 2.5	97.2 ± 1.1	99.0 ± 0.5	99.1 ± 0.6
	90°	61.6 ± 6.5	78.3 ± 4.7	93.6 ± 1.7	96.3 ± 1.1	99.3 ± 0.4	99.5 ± 0.5	99.7 ± 0.3	100 ± 0

positions (90° and 270°) [7] in the vertical meridian is evident: vertical motion perception is either near 100% or is much superior when compared to the other positions. A value of 100% means that the participant perceived vertical apparent motion for every stimulus presented.

From these values we estimated the psychometric fits using a logistic function from Palamedes toolbox [102]. All parameters were set as described in section 3.4. Figure 4.2 presents the psychometric functions for participants 03, 06 and 14 as well as the interpolated parity ratios (point where the percentage of vertical motion is equal to 50 % for each position, for both left and right hemifields. The average hemifield PR was also included. The psychometric curves for the rest of the participants can be found in the appendix (figures A.1 and A.2).

All the psychometric curves had a deviance's p-value (see section 3.4) higher

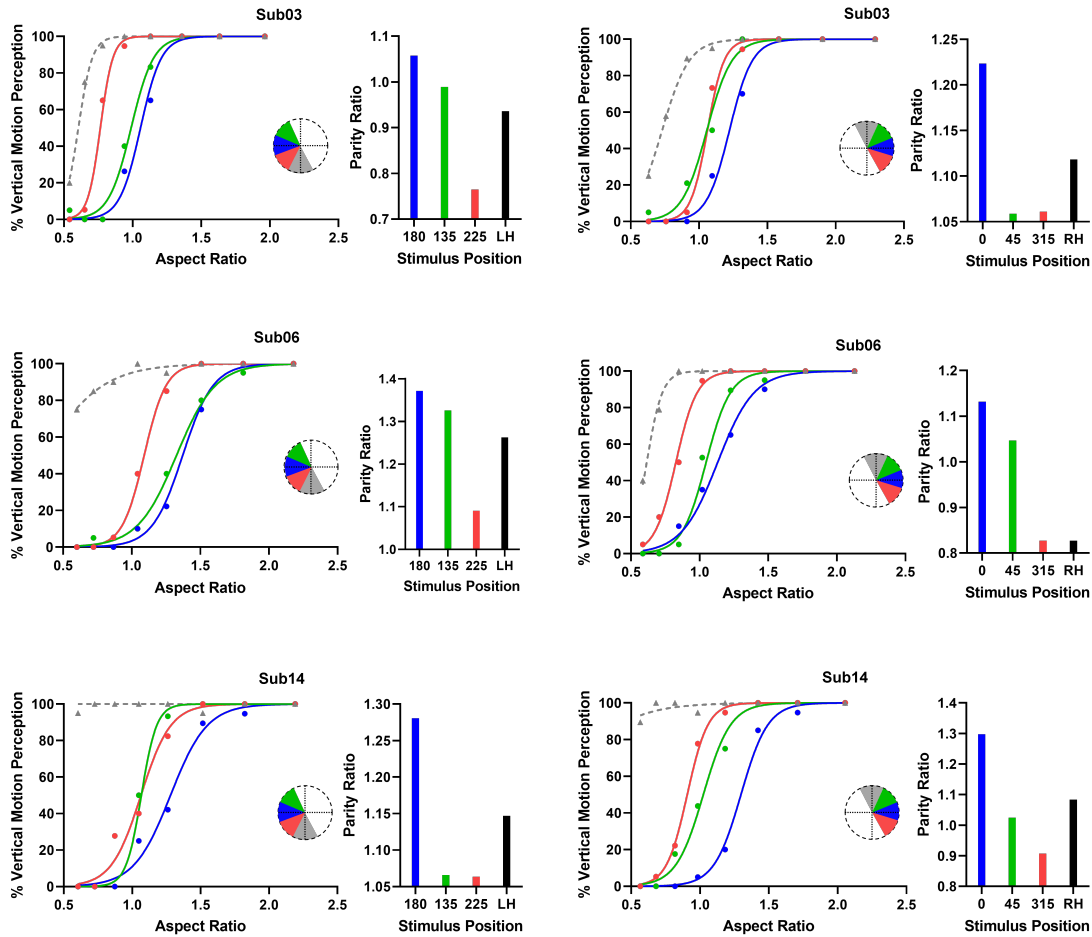


**Figure 4.2: Psychometric function and respective interpolated parity ratios for left and right hemifields of participants 03, 06 and 14.** The psychometric fits represent the percentage of vertical motion perception relatively to the aspect ratio. Rows correspond to data of different participants. Left and Right columns correspond to estimates for left and right visual field, respectively. Dots correspond to the 8 aspect ratios used during MoCS task. Blue color represents the middle positions ( $0^\circ$  and  $180^\circ$ ), the green color corresponds to top positions ( $45^\circ$  and  $135^\circ$ ), the red color represents the bottom positions ( $315^\circ$  and  $225^\circ$ ) and the gray color corresponds to control positions ( $90^\circ$  and  $270^\circ$ ). The bar charts display the relationship between the parity ratios extracted from the psychometric curves and the stimulus positions. Parity ratio (PR) is determined by taking the aspect ratio where the logistic function estimates a value of 50% vertical motion perception. The LH and RH bars refer to the average parity ratio of the left and right hemifields, respectively.

than 0.05 meaning that all fits were considered acceptable. The average p-value for all fits was 0.413. The resultant PR's data for all participants was organized per stimulus positions for both left and right hemifields and it is depicted in figure 4.3.

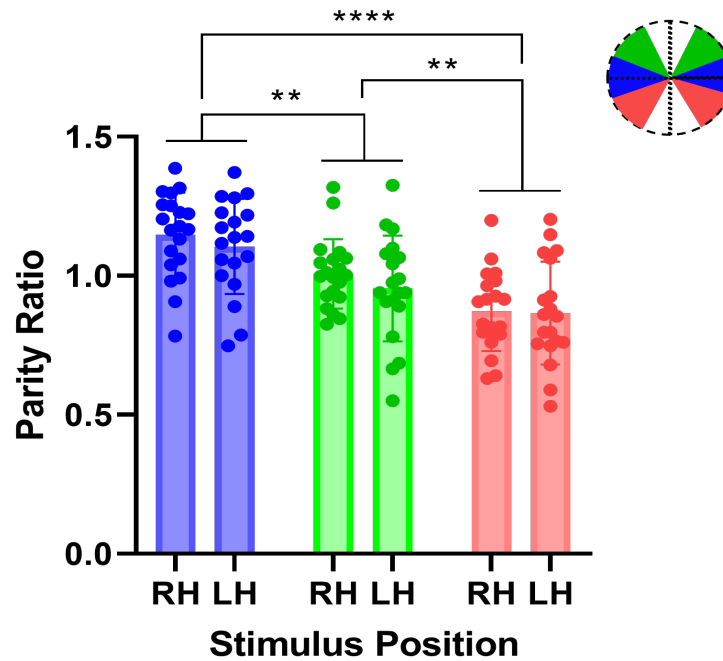


**Figure 4.3: Distribution of parity ratios for all participants per stimulus position.** Comparison between the parity ratios from the left (LH) and right (RH) hemifields for the middle (blue), top (green) and bottom (red) positions. Bars depict mean  $\pm$  SEM. Circles depict individual values from each participant. \*\*  $p < 0.01$ , \*\*\*\*  $p < 0.0001$ , Holm-Sidak corrected.

From figure 4.3, it is already possible to verify the already expected large interindividual variability of the PR's values [7], as the subject representative dots are scattered over a large interval (e.g. minimum of 0.75, maximum of 1.37 for midline position of the left hemifield; average range of 0.63 across all conditions).

In order to analyse the influence of the stimulus position on the participant's PRs and whether there is a difference between hemifields, a two-way repeated measures analysis of variance (ANOVA) was performed. Participant 07 did not perform the experiment for the left hemifield and therefore was not considered in this statistical analysis. The hemifield effect resulted in no significant difference in the average parity ratio between the right ( $1.015 \pm 0.081$ ) and left hemifields ( $0.975 \pm 0.070$ ;  $F(1,18)=1.446$ ,  $p=0.2448$ ). This means that the hemifield where the stimulus was displayed did not affect its motion perception. On the other hand, the main effect of stimulus position was highly significant ( $F(2,36)=39.21$ ,  $p < 0.0001$ ) indicating that stimulus position contributed significantly to differences in the parity ratio, hence

perception is differently biased across the tested positions. As expected, the interaction between stimulus position and hemifield was not significant ( $F(2,36)=0.445$ ,  $p=0.644$ ) thus the stimulus position effect was similar in both hemifields. Post hoc analyses using the Tukey's multiple comparisons test indicated that the average parity ratio, in the right hemifield, was significantly higher for the horizontal meridian position ( $1.156 \pm 0.034$ ) when compared to both top ( $1.011 \pm 0.028$ ; Tukey's post-hoc test,  $p=0.0007$ ) and bottom ( $0.877 \pm 0.032$ ; Tukey's post-hoc test,  $p<0.0001$ ) positions. The same happens in the left hemifield, with the average parity ratio being significantly higher for the horizontal meridian position ( $1.105 \pm 0.039$ ) than it was for both top ( $0.955 \pm 0.044$ , Tukey's post-hoc test,  $p=0.0005$ ) and bottom ( $0.865 \pm 0.043$ ; Tukey's post-hoc test,  $p<0.0001$ ) positions. Additionally, the average parity ratio was significantly higher in the top positions than it was in the bottom positions for both right,  $p=0.0020$  and left hemifields,  $p=0.0455$ .

A higher PR means that the stimulus configuration, for which the participant perceives vertical or horizontal apparent motion with equal probability, has a higher width/height ratio. In other words, a PR higher than 1 indicates that the horizontal distance between the stimulus dots has to be greater than the vertical distance for the point of perceptual equivalence to be reached. Likewise, comparing PR values relative to each other, a higher PR value means that the horizontal distance has to be greater to reach a point of equiprobable vertical/horizontal motion perception. Therefore, we can say that a larger PR indicates a higher tendency to perceive horizontal apparent motion. The results presented are indicative of a readiness of the visual system to interpret horizontal motion when the ambiguous stimulus is displayed along the horizontal meridian of both hemifields.

#### 4.2.1.1 Eyetracking Analysis

As a control analysis for the influence of gaze positions/eye movements a second psychometric fit was performed for 18 of the 20 participants using the criteria described in section 3.5.2 for selecting trials with strict gaze control within a window around fixation. Eye tracking data of 14 out of the 18 participants met the strict criteria set to ensure proper fixation while also providing a sufficient number of trials for reliable psychophysical fits. Figure 4.4 shows the mean fixation density plots produced by the 5 run eye tracking data from participants 03, 06 and 14, for each hemifield. The fixation density plots for all 14 participants can be found in the appendix (figures A.3 and A.4).

All the psychometric curves estimated in this manner had a deviance's p-value (see section 3.4) higher than 0.05 which means that all were considered acceptable.

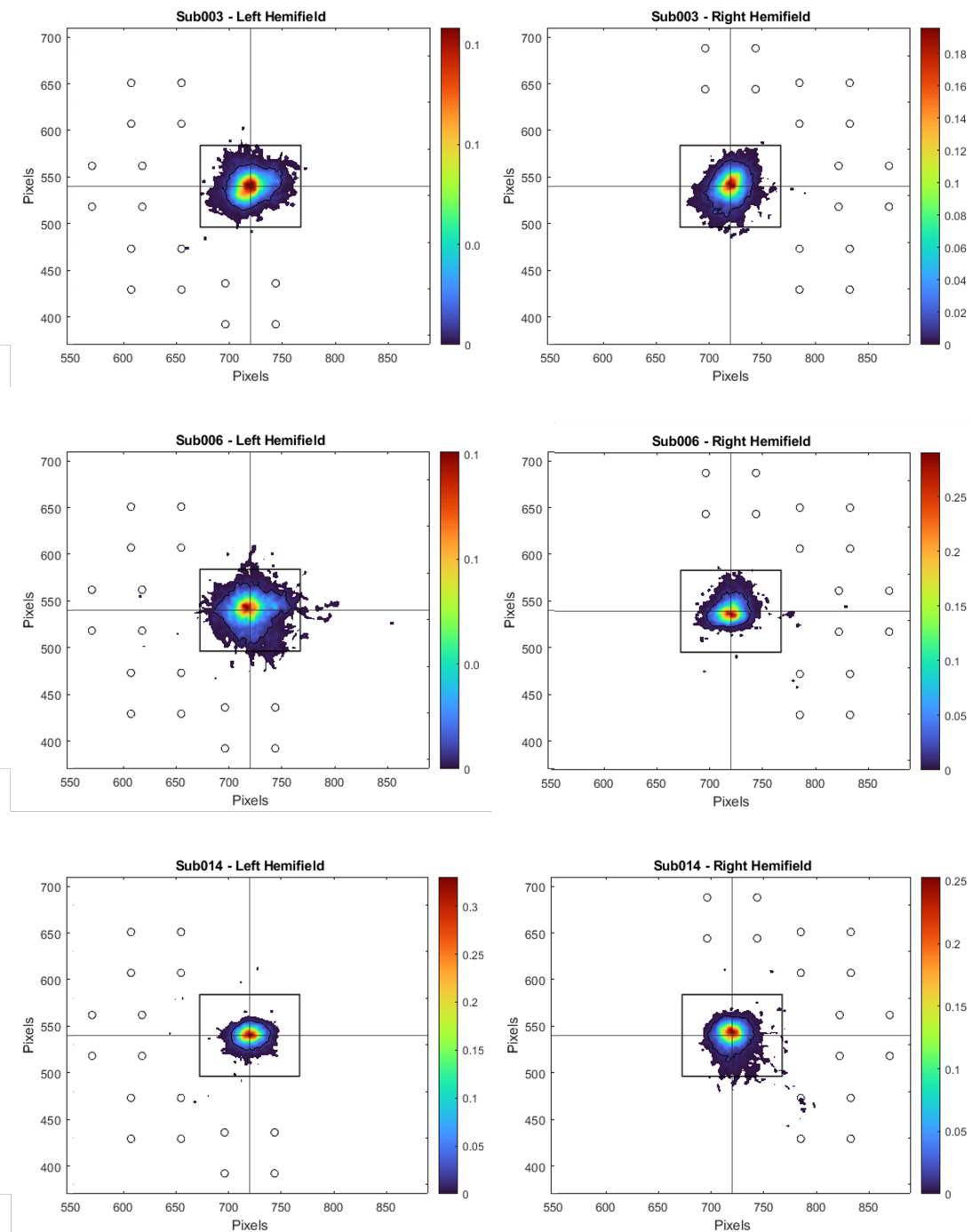


**Figure 4.4: Average fixation density plots for the left and right hemifields of participants 03, 06 and 14.** The screen's centre is given by the intersection of axes  $y = 1080/2$  px and  $x = 1440/2$  px. The window's dimensions, at the centre of the plots, are described in section 3.5.2. The black contour contains 90% of the gaze position data. Black circles represent the stimulus positions during the visual task.

The average p-value for all fits was 0.467. The PR data obtained from the Fixation Controlled (FC) psychometric functions was compared, for both hemifields, to the one obtained by the original fits. As can be seen in Figure 4.5, the PRs obtained for all conditions, namely middle, top and bottom positions for left and right hemispheres, using a strict fixation criteria, were identical to the original ones. All values for the left and right hemifields can be found in table 4.3 and 4.4, respectively.

**Table 4.3: Average parity ratios for the middle, top and bottom positions of the right hemisphere, for both the original and the fixation controlled psychometric functions.** Values correspond to mean  $\pm$  SEM of 14 participants.

	<b>Middle</b>	<b>Top</b>	<b>Bottom</b>
<b>Original</b>	1.092 $\pm$ 0.049	0.983 $\pm$ 0.055	0.871 $\pm$ 0.050
<b>Fixation Controlled</b>	1.089 $\pm$ 0.051	0.993 $\pm$ 0.055	0.874 $\pm$ 0.050

**Table 4.4: Average parity ratios for the middle, top and bottom positions of the right hemisphere, for both the original and the fixation controlled psychometric functions.** Values correspond to mean  $\pm$  SEM of 14 participants.

	<b>Middle</b>	<b>Top</b>	<b>Bottom</b>
<b>Original</b>	1.139 $\pm$ 0.044	1.004 $\pm$ 0.030	0.854 $\pm$ 0.037
<b>Fixation Controlled</b>	1.143 $\pm$ 0.050	0.987 $\pm$ 0.039	0.850 $\pm$ 0.040

In order to analyse the influence of the stimulus position on the PRs from the FC psychometric functions and whether there is a difference between hemifields, a two-way repeated measures analysis of variance (ANOVA) was performed. The hemifield effect yielded an F ratio of  $F(1,13)=0,04725$ ,  $p=0,8313$ , indicating that there was no significant difference in the average parity ratio between the right ( $0.994 \pm 0.085$ ) and left ( $0.985 \pm 0.062$ ) hemifields. Once again, the hemifield where the stimulus was displayed did not affect its motion perception. Moreover, the same differences in PR due to stimulus position effect were found in this new analysis ( $F(2,26)= 24.39$ ,  $p<0.0001$ ). Post-hoc analyses indicated that the average parity ratio for horizontal meridian positions ( $1.116 \pm 0.027$ ), of both hemifields, was significantly higher when compared to both top ( $0.990 \pm 0.003$ ; Tukey's post-hoc test,  $p=0.0051$ ) and bottom ( $0.862 \pm 0.012$ ; Tukey's post-hoc test,  $p<0.0001$ ) positions. Additionally, the average parity ratio was significantly higher in the top positions than it was in the bottom positions (Tukey's post-hoc test,  $p<0.0045$ ).

These results imply that, independently from the hemifield, the differences observed for distinct positions is unlikely to result from eye movements. However, even though gaze position was controlled as a surrogate for ocular movements, measurement of saccades was not conducted in this study and, therefore, can be considered

as a limitation. Moreover, for all 14 participants, average gaze position during the task was confirmed to fall within the central fixation point, confirming that all participants were adhering to the instructions given.

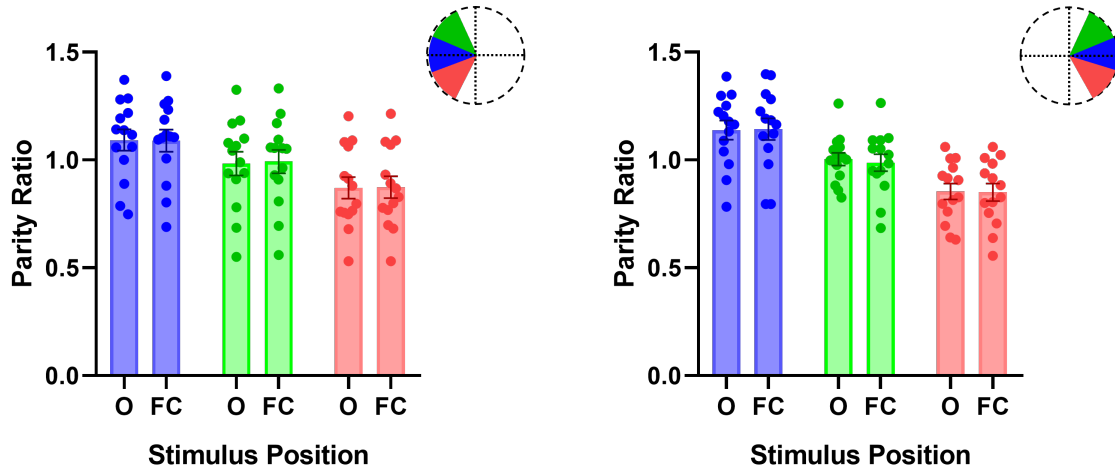


**Figure 4.5: Distribution of parity ratio's values for all 14 participants per stimulus position.** Comparison between the PR's values from the original (O) and fixation controlled (FC) psychometric fits for the middle (blue), top (green) and bottom (red) positions, in both hemifields.

## 4.2.2 Experiment 2

Despite the evident horizontal perceptual bias in the horizontal midline, this finding had not been previously reported, to our knowledge, and thus the reason behind it was unclear. More specifically, we wondered what regions of the visual cortical map and perhaps, what anatomical constraints could be causing this effect. As a first attempt to unveil the origin of such effect, an experiment was carried out with varying levels of stimulus' contrast to engage mechanisms that might be operating more at the early visual processing. Due to the fact that retinal responses are extremely sensitive to all contrast levels, contrast is an appropriate parameter for investigation. Therefore, contrast response can be used as a tool to explore to what extent activation in a given visual area is related to the subject's perceptual performance. This experiment was based in functional Magnetic Resonance Imaging (fMRI) studies that used visual contrast variation to study neuronal activity in the early visual cortex [105–107].

As in experiment 1, the MoCS task resulted in a set of eight vertical motion percept proportions, one value for each aspect ratio and, in this case, a set for each one of the five Michelson Contrasts (MCs) tested (see section 3.3.2). This sets were used to calculate the PR at a single location, the horizontal meridian. Table 4.5



presents the MoCS task results for participants 02, 21 and 22 as well as the average for all participants. The aspect ratios were selected based on each participant’s first estimate of the PR obtained by the MoL (see section 3.3) which corresponds to the 4<sup>o</sup> ratio on the tables. Knowing from experiment 1 that the hemifield where the stimulus is displayed does not affect the horizontal bias observed, in experiment 2, only one hemifield was tested. Participants 01, 02, 21 and 24 viewed the stimuli in the left hemifield while participants 22, 23 and 25 viewed the stimuli in the right hemifield.

**Table 4.5: Percentage of vertical motion perception values for participants 02, 21 and 22 as well as the average for all participants, for each Michelson contrast used in the visual stimulus.**

Participant	MC(%)	1 <sup>o</sup> Ratio	2 <sup>o</sup> Ratio	3 <sup>o</sup> Ratio	4 <sup>o</sup> Ratio	5 <sup>o</sup> Ratio	6 <sup>o</sup> Ratio	7 <sup>o</sup> Ratio	8 <sup>o</sup> Ratio
02	5	0	5.0	0	0	40.0	80.0	100	100
	10	0	0	0	5.0	68.4	80.0	100	100
	20	0	0	0	5.0	55.0	100	100	100
	40	0	0	15.0	0	50.0	100	100	100
	80	0	0	5.0	20.0	70.0	95.0	100	100
21	5	0	0	0	10.5	25.0	60.0	100	100
	10	0	0	5.3	10.0	25.0	70.0	100	100
	20	0	0	0	15.0	44.4	85.0	100	100
	40	0	0	10.0	21.1	45.0	90.0	100	100
	80	0	0	10.0	26.3	25.0	75.0	95.0	100
22	5	0	5.0	25.0	63.2	90.0	95.0	100	100
	10	0	15.8	45.0	55.0	90.0	90.0	100	100
	20	0	10.0	10.0	40.0	70.0	90.0	100	100
	40	0	5.3	0	57.9	75.0	94.4	100	100
	80	0	5.0	15.8	50.0	55.0	90.0	100	100
Mean $\pm$ SEM	5	4.5 $\pm$ 4.5	7.9 $\pm$ 5.4	16.0 $\pm$ 7.2	29.4 $\pm$ 8.5	62.2 $\pm$ 9.1	73.6 $\pm$ 6.6	91.5 $\pm$ 5.1	98.3 $\pm$ 1.1
	10	2.4 $\pm$ 2.4	15.4 $\pm$ 8.0	17.3 $\pm$ 6.1	29.8 $\pm$ 7.5	64.3 $\pm$ 8.3	81.4 $\pm$ 4.7	94.2 $\pm$ 3.5	98.4 $\pm$ 1.1
	20	2.9 $\pm$ 2.2	18.2 $\pm$ 8.4	13.0 $\pm$ 7.8	29.9 $\pm$ 7.6	58.9 $\pm$ 7.1	85.8 $\pm$ 6.5	95.4 $\pm$ 2.8	99.3 $\pm$ 0.7
	40	2.8 $\pm$ 2.1	7.8 $\pm$ 5.2	21.9 $\pm$ 9.4	36.4 $\pm$ 8.7	60.6 $\pm$ 6.5	82.7 $\pm$ 6.6	96.0 $\pm$ 2.2	96.8 $\pm$ 2.3
	80	1.3 $\pm$ 1.3	13.7 $\pm$ 8.7	20.7 $\pm$ 7.6	35.4 $\pm$ 4.6	49.7 $\pm$ 5.8	82.4 $\pm$ 5.5	90.9 $\pm$ 5.3	96.8 $\pm$ 2.1

Like for experiment 1, these results allowed us to estimate the psychometric fits under different contrasts using a logistic function [102]. All parameters were set as described in section 3.4. Figure 4.6 presents the psychometric functions for participants 02, 21 and 22 as well as the interpolated PRs for each Michelson contrast. The average hemifield PR was also included. The psychometric curves for the rest of the participants can be found in the appendix (figure A.5).

All the psychometric curves had a deviance’s p-value (see section 3.4) higher than 0.05 which means that all fits were considered acceptable. The average p-value for all fits was 0.478. The resultant PR’s data for all participants was organized per MC independently of the hemifield and is depicted in figure 4.7.

A first observation of figure 4.7 seems to indicate that there is no significant differences between the PR means of the five MCs. The average PRs values for the 5%, 10%, 20%, 40% and 80% MC were  $1.142 \pm 0.066$ ,  $1.116 \pm 0.047$ ,  $1.116 \pm 0.055$ ,  $1.114 \pm 0.048$ ,  $1.149 \pm 0.029$ , respectively. To better understand if different

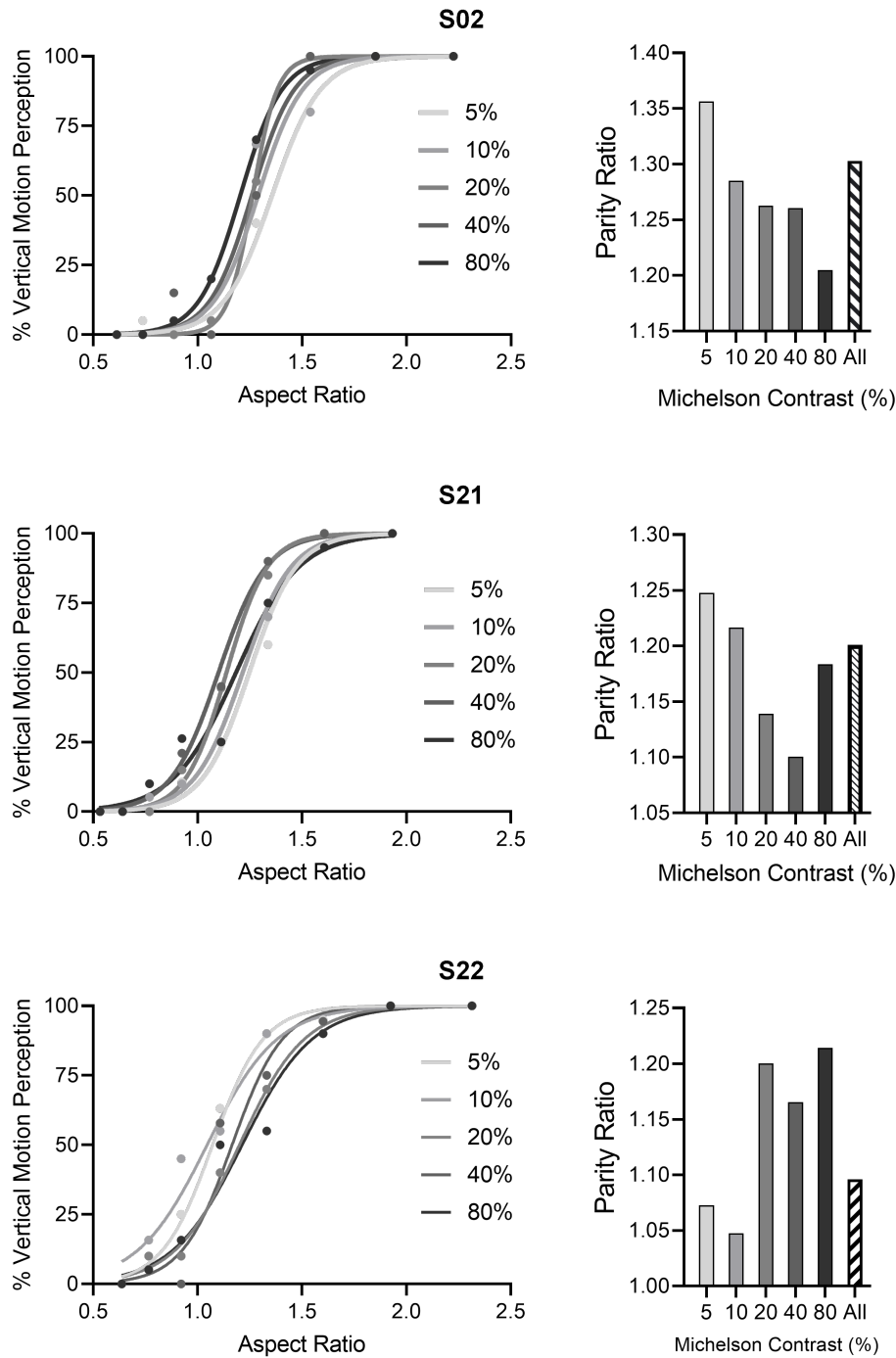


**Figure 4.6: Psychometric functions and respective interpolated parity ratios for the left hemifield of participants 02 and 21 and right hemifield of participant 22.** The psychometric fits represent the percentage of vertical motion perception in relation to the aspect ratio. The dots correspond to the 8 aspect ratios used. The bar charts display the relationship between the parity ratios extracted from the psychometric curves and the five stimulus Michelson contrasts (%). Parity ratios were determined by taking the aspect ratio where the logistic function has a value of 50% vertical motion perception. The "All" bars refer to the average parity ratio of the hemifield being tested.

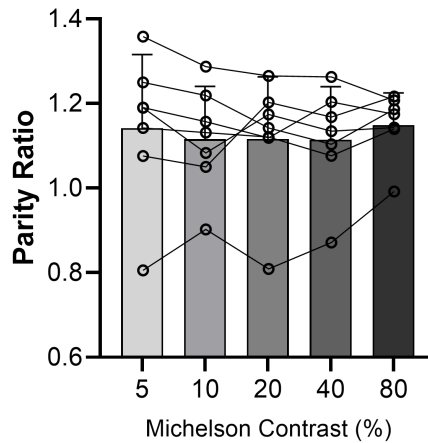


**Figure 4.7: Distribution of the parity ratio’s values for all participants per Michelson contrast independently of the hemifield.** Bars depict mean  $\pm$  *SEM*. Circles depict individual values from each participant.

levels of contrast would alter the PR values for the 7 participants and, hence, influence the participant’s motion perception, a one-way repeated measures analysis of variance (ANOVA) was performed. The effect of contrast was non significant ( $F(2,14)=0.5811$ ,  $p=0.5918$ ).

These results are indicative that the horizontal bias effect described before might not be attributed to early visual cortical processing given their contrast insensitivity. Otherwise, it would be expected that, for different contrasts, the PR values would be different as well, i.e., it would cause a change in the participant’s perception of apparent motion. As visual signals pass through the different cortical regions of the visual pathway (see section 1.2.1), their sensitivity to contrast information decreases. Therefore primary visual cortex (V1) is the most sensitive cortical region to contrast, which means that small variations of contrast would impact the motion perception of the SAM which clearly does not happen. As will be discussed, our first hypothesis was that anatomical constraints in the primary visual cortex might be behind this effect.

### 4.3 General Discussion

The current work aimed at studying ambiguous motion perception across the visual field to confirm a novel anisotropic effect and offer potential insights into the motion correspondence problem. Starting from a preliminary study, we devised a protocol to study how solutions to ambiguous motion are biased in more than only the previously described vertical bias in the centre of the visual field/vertical

meridian. We identified a second type of motion anisotropy within the horizontal meridian that could relate perceptual outcomes to visual cortical structure.

The novelty of this effect is striking, as in our study it was quite robust and reliably observed in a majority of subjects. To our knowledge this effect has not been previously reported and thus holds particular importance for the study of ambiguity in vision, as it may arise from mechanisms that despite having a significant effect in visual perception might have been overlooked until now. Moreover, as the SAM is frequently employed in the study of cognition and of brain signals of perceptual decision, the presence of such effect may even account for possible confounds in previous studies. Since the first study describing the metastable stimulus creating competing perceptions of apparent motion, stimulus position was observed to influence movement perception. The seminal report by Gengerelli [108] revealed that the SAM displayed across both hemispheres, i.e. in central fixation, was much more likely to be perceived describing vertical motion than horizontal. This is a robust effect that appears to hinge on the necessity of interhemispheric transfer of information for horizontal motion to be perceived while only intrahemispheric signals are required for vertical motion, when SAM is displayed at the centre of the visual field [90]. Signal degradation or delay through callosal fibers are likely the main reason for this vertical bias. In fact, Genç and colleagues [7] have provided compelling evidence using tractography, that correlates the structure of interhemispheric fibers of the corpus callosum with the interindividual variance in the SAM's motion perception. On the other hand, the anisotropy towards horizontal motion described here appears to have eluded previous studies. Chauduri and Glaser [90] described in detail the anisotropy resulting from central display of the metastable figure, but surprisingly only reported a small vertical, not horizontal, bias in the horizontal meridian. More recently, Boeykens [6] performed an extensive mapping of SAM perceptual dynamics related to spatial distance, temporal distance and also spatial location. Nonetheless, the authors report no horizontal bias at the horizontal midline. The described studies and the current work corroborate 1) the visual system's adherence to Ullmans [109] minimal mapping theory, i.e. when faced with a correspondence problem, motion is more likely perceived across the smaller distance [6, 90], and 2) the anisotropy arising from the brain favours intrahemispheric solutions [7, 90, 108]. We believe the effect of horizontal bias along the horizontal meridian might have been reduced, and hence overlooked, due to differences in experimental protocols that could have diminished effects of competition, as will be described. Most studies of ambiguous apparent motion relate inter-element distances with the likelihood of perceiving motion in a particular direction. This translates to vertical and hor-

horizontal perception being dominant for figures with greater vertical proximity, i.e. small h/v aspect ratio, and greater horizontal proximity, i.e. high h/v aspect ratio, respectively. However, most studies derive this relation between distance and perception using fixed distances for one of the axis while increasing or decreasing the distance of the other. This has overall the same effect of biasing perception towards the smallest distance but measures competition between stimuli with significantly different element distances. In other words, the stimuli used are described by a varying aspect ratio but also vary over a wide array of sizes [6, 7, 90, 99]. In the current work that is not the case. In order to avoid displaying figures encompassing varying areas and engaging more peripheral or more central vision due to disparate sizes, SAM stimuli were created in a way that all figures had the same area regardless of its aspect ratio. This might have created optimal conditions to study the competition between highly plausible solutions that, in the absence of ambiguity from presenting two pairs of alternating dots, would result in equally strong apparent motion perception. In this manner, we were able to confirm the central vertical bias and to identify two other sources of bias in ambiguous motion perception: 1) an evident preference towards horizontal motion in the horizontal meridian; and 2) a bias towards horizontal motion in the upper visual field when compared to the lower visual field. These findings do not support simply an increase in preference to horizontal motion as one goes from lower visual field to upper: the horizontal midline effect is still higher when compared to the upper visual field. More likely, this represents a bias that is more pronounced in the azimuth and then has a fall off, albeit asymmetric, as one moves up or down on the visual field. While this phenomenon mirrors the vertical bias in the vertical meridian its effect is of a smaller magnitude: PRs varied with stimuli dimensions within 20-35% among the single visual field conditions, i.e. distances between dots had to change between 20 to 35% to compensate for direction bias and reach equiprobability. On the other hand, in the vertical meridian the point of equiprobable perception requires a vertical distance at least 50% larger than the horizontal distance. This suggests that, whatever mechanisms operate to solve the correspondence problem and interpret motion [110, 111], the solutions can be more or less biased based on either shortcomings of the brain mechanisms of integrating information along a particular path [7, 112], or a built-in preference towards particular directions of motion [113–116].

First, let's consider the hypothesis that within a single visual hemisphere there are obstacles to manifesting a particular Gestalt solution, i.e. integrating apparent motion as if the dots cross the horizontal meridian. There are in fact aspects of the early visual cortex organization that could account for this cortical behaviour. For

instance, while there is continuity of the cortical sheet in V1, unlike areas V2 and V3 downstream, the primary visual cortex is anatomically separated by a sulcal structure, the calcarine sulcus. This structure does not represent a discontinuity like the hemispheric separation that requires callosal connection for interhemispheric communication, but can still correlate with microstructural idiosyncrasies that create a barrier to signal flow across the lower and upper visual field. Differences in receptive field shape and orientation in the early visual cortex are still an undetermined topic [117, 118] but, V1, V2 and V3 have been found to respond more strongly to centripetal and centrifugal motion [115]. This radial motion direction bias is likely to be originated from anisotropies in long range horizontal connections, which are also believed to play a role in the filling-in of apparent motion [119, 120]. In fact, there is growing interest of signals carried by cortical horizontal projections in the reconstructive aspects of apparent motion [121]. Our findings are consistent with this directional anisotropies of motion sensitivity in the visual cortex.

A focus on anatomical constraints and cortical structural-functional correlations is not without merit, as a quadrant arrangement of visual cortical areas [95, 96] is also aligned with the results obtained in this thesis. While V2 and V3 represent visual quadrants, with the upper and lower visual fields being anatomically flanked by V1, this does not happen to V1 as the upper and lower visual fields are contiguous in each hemifield. In the second experiment, the metric of parity ratio revealed to be insensitive to the variations of the visual stimulus contrast. It is known that there is a gradual trend of increasing contrast invariance moving from area V1, which have high sensitivity to contrast changes, to high order visual areas along the ventral stream [105]. Therefore, the result obtained might be indicative that the horizontal motion effect reported before does not have its initial locus in the primary visual cortex but in cortical areas with quadrant representations whose anatomical breaks correspond to the horizontal meridian.

## Conclusion and Future perspectives

The work presented in this thesis provided us tools to better comprehend how ambiguous stimulus' positioning in the visual field affects the perception of apparent motion. Two main experiments were designed following a rigorous methodology that included 1) the use of a Stroboscopic Alternative Motion (SAM) capable of providing a clear perceptual competition by varying its aspect ratio, and 2) a strict eye tracking analysis that supported the viability of the results obtained. Results from the first experiment contributed greatly to the psychophysics literature as it allowed us to present solid evidence of an unreported perceptual effect occurring when ambiguous stimuli of apparent motion are presented over the horizontal meridian of the visual field. Moreover, we were able to reproduce the vertical perception bias when an ambiguous stimulus of apparent motion, such as the SAM, is presented along the vertical meridian of the visual field.

Despite the undeniable horizontal perception effect observed, its origin remained unknown with many possibilities being considered in the General Discussion (section 4.3). Nonetheless, the results from the second experiment revealed that this effect is insensitive to stimulus' contrasts variation. Thus, it is unlikely that its emergence happens in the primary visual cortex (V1).

In the future, different experiments can be made to better comprehend what visual cortical mechanisms might be behind the horizontal bias effect reported in this thesis. Namely, studying the dependence of this effect on apparent motion orientation could reveal whether this is a result of an overall radial motion bias or orientation bias of visual cortical areas. If the effect of direction bias and a putative intra-quadrantic field bias could be disentangled, the hypothesis that neural activity binds together tokens within a visual quadrant could be further explored. Additionally, the introduction of functional Magnetic Resonance Imaging (fMRI) would be an important tool to better understand the retinotopical positioning of the SAM in the primary visual cortex, allowing to test if anatomical constraints such as

the calcarine sulcus could be causing the horizontal bias effect. By combining the precision of current retinotopic mapping methods with protocols of fMRI to assess activity related to path reconstruction, one could study the neural correlates of this perceptual phenomenon.



# Bibliography

- [1] M. d. S. Santos, *Brain signals of perceptual inference: the role of oscillations in interpreting ambiguous stimuli*. PhD thesis, Universidade de Coimbra, 2020.
- [2] B. G. Breitmeyer, J. G. May, and M. C. Williams, “Spatial frequency and contrast effects on percepts of bistable stroboscopic motion,” *Perception & Psychophysics*, vol. 44, no. 6, pp. 525–531, 1988.
- [3] H. S. Hock, J. S. Kelso, and G. Schöner, “Bistability and hysteresis in the organization of apparent motion patterns,” *Journal of Experimental Psychology: Human Perception and Performance*, vol. 19, no. 1, p. 63, 1993.
- [4] H. S. Hock, K. Kogan, and J. K. Espinoza, “Dynamic, state-dependent thresholds for the perception of single-element apparent motion: Bistability from local cooperativity,” *Perception & psychophysics*, vol. 59, no. 7, pp. 1077–1088, 1997.
- [5] P. Sterzer and A. Kleinschmidt, “A neural signature of colour and luminance correspondence in bistable apparent motion,” *European Journal of Neuroscience*, vol. 21, no. 11, pp. 3097–3106, 2005.
- [6] C. Boeykens, J. Wagemans, and P. Moors, “Perception of the ambiguous motion quartet: a stimulus-observer interaction approach,” *Journal of Vision*, vol. 21, no. 13, pp. 12–12, 2021.
- [7] E. Genç, J. Bergmann, W. Singer, and A. Kohler, “Interhemispheric connections shape subjective experience of bistable motion,” *Current Biology*, vol. 21, no. 17, pp. 1494–1499, 2011.
- [8] M. M. Schira, C. W. Tyler, and M. G. Rosa, “Brain mapping: the (un) folding of striate cortex,” *Current Biology*, vol. 22, no. 24, pp. R1051–R1053, 2012.
- [9] B. A. Wandell, S. O. Dumoulin, and A. A. Brewer, “Visual field maps in human cortex,” *Neuron*, vol. 56, no. 2, pp. 366–383, 2007.

- 
- [10] T. Huff, N. Mahabadi, and P. Tadi, “Neuroanatomy, visual cortex,” in *StatPearls [Internet]*, StatPearls Publishing, 2021.
- [11] D. Purves, G. J. Augustine, D. Fitzpatrick, W. Hall, A.-S. LaMantia, and L. White, *Neurosciences*. De Boeck Supérieur, 2019.
- [12] D. H. Hubel and T. N. Wiesel, “Shape and arrangement of columns in cat’s striate cortex,” *The Journal of physiology*, vol. 165, no. 3, p. 559, 1963.
- [13] A. Anzai, X. Peng, and D. C. Van Essen, “Neurons in monkey visual area v2 encode combinations of orientations,” *Nature neuroscience*, vol. 10, no. 10, pp. 1313–1321, 2007.
- [14] M. A. Goodale, “Transforming vision into action,” *Vision research*, vol. 51, no. 13, pp. 1567–1587, 2011.
- [15] R. F. Dougherty, V. M. Koch, A. A. Brewer, B. Fischer, J. Modersitzki, and B. A. Wandell, “Visual field representations and locations of visual areas v1/2/3 in human visual cortex,” *Journal of vision*, vol. 3, no. 10, pp. 1–1, 2003.
- [16] Y. Ejima, S. Takahashi, H. Yamamoto, M. Fukunaga, C. Tanaka, T. Ebisu, and M. Umeda, “Interindividual and interspecies variations of the extrastriate visual cortex,” *Neuroreport*, vol. 14, no. 12, pp. 1579–1583, 2003.
- [17] S. Pitzalis, C. Galletti, R.-S. Huang, F. Patria, G. Comitteri, G. Galati, P. Fattori, and M. I. Sereno, “Wide-field retinotopy defines human cortical visual area v6,” *Journal of Neuroscience*, vol. 26, no. 30, pp. 7962–7973, 2006.
- [18] U. Hasson, I. Levy, M. Behrmann, T. Hendler, and R. Malach, “Eccentricity bias as an organizing principle for human high-order object areas,” *Neuron*, vol. 34, no. 3, pp. 479–490, 2002.
- [19] J. W. Brascamp and S. K. Shevell, “The certainty of ambiguity in visual neural representations,” *Annual Review of Vision Science*, vol. 7, pp. 465–486, 2021.
- [20] J. Brascamp, P. Sterzer, R. Blake, and T. Knapen, “Multistable perception and the role of the frontoparietal cortex in perceptual inference,” *Annu Rev Psychol*, vol. 69, pp. 77–103, 2018.
- [21] D. H. Arnold, P. M. Grove, and T. S. Wallis, “Staying focused: A functional account of perceptual suppression during binocular rivalry,” *Journal of Vision*, vol. 7, no. 7, pp. 7–7, 2007.

- 
- [22] B. A. Doshier, G. Sperling, and S. A. Wurst, “Tradeoffs between stereopsis and proximity luminance covariance as determinants of perceived 3d structure,” *Vision research*, vol. 26, no. 6, pp. 973–990, 1986.
- [23] J.-Y. Hsiao, Y.-C. Chen, C. Spence, and S.-L. Yeh, “Assessing the effects of audiovisual semantic congruency on the perception of a bistable figure,” *Consciousness and Cognition*, vol. 21, no. 2, pp. 775–787, 2012.
- [24] V. Conrad, M. P. Vitello, and U. Noppeney, “Interactions between apparent motion rivalry in vision and touch,” *Psychological science*, vol. 23, no. 8, pp. 940–948, 2012.
- [25] R. Sundareswara and P. R. Schrater, “Perceptual multistability predicted by search model for bayesian decisions,” *Journal of vision*, vol. 8, no. 5, pp. 12–12, 2008.
- [26] K. Maruya, E. Yang, and R. Blake, “Voluntary action influences visual competition,” *Psychological Science*, vol. 18, no. 12, pp. 1090–1098, 2007.
- [27] D. A. Leopold, M. Wilke, A. Maier, and N. K. Logothetis, “Stable perception of visually ambiguous patterns,” *Nature neuroscience*, vol. 5, no. 6, pp. 605–609, 2002.
- [28] J. Pearson and J. Brascamp, “Sensory memory for ambiguous vision,” *Trends in cognitive sciences*, vol. 12, no. 9, pp. 334–341, 2008.
- [29] J. Pearson, C. W. Clifford, and F. Tong, “The functional impact of mental imagery on conscious perception,” *Current Biology*, vol. 18, no. 13, pp. 982–986, 2008.
- [30] K. Schmack, V. Weilhhammer, J. Heinzle, K. E. Stephan, and P. Sterzer, “Learning what to see in a changing world,” *Frontiers in human neuroscience*, vol. 10, p. 263, 2016.
- [31] M. Di Luca, M. O. Ernst, and B. T. Backus, “Learning to use an invisible visual signal for perception,” *Current Biology*, vol. 20, no. 20, pp. 1860–1863, 2010.
- [32] K. Schmack, A. G.-C. de Castro, M. Rothkirch, M. Sekutowicz, H. Rössler, J.-D. Haynes, A. Heinz, P. Petrovic, and P. Sterzer, “Delusions and the role of beliefs in perceptual inference,” *Journal of Neuroscience*, vol. 33, no. 34, pp. 13701–13712, 2013.

- 
- [33] P. Sterzer, C. Frith, and P. Petrovic, “Believing is seeing: expectations alter visual awareness,” *Current Biology*, vol. 18, no. 16, pp. R697–R698, 2008.
- [34] R. B. Lotto, D. Purves, and S. Nundy, “Why we see what we do: A probabilistic strategy based on past experience explains the remarkable difference between what we see and physical reality,” *American Scientific*, vol. 90, pp. 236–43, 2002.
- [35] D. Purves, W. T. Wojtach, and R. B. Lotto, “Understanding vision in wholly empirical terms,” *Proceedings of the National Academy of Sciences*, vol. 108, no. supplement\_3, pp. 15588–15595, 2011.
- [36] D. Purves, R. Beau Lotto, S. Mark Williams, S. Nundy, and Z. Yang, “Why we see things the way we do: evidence for a wholly empirical strategy of vision,” *Philosophical Transactions of the Royal Society of London. Series B: Biological Sciences*, vol. 356, no. 1407, pp. 285–297, 2001.
- [37] A. Gilchrist, *Seeing black and white*. Oxford University Press, 2006.
- [38] E.-J. Chichilnisky and B. A. Wandell, “Photoreceptor sensitivity changes explain color appearance shifts induced by large uniform backgrounds in dichoptic matching,” *Vision research*, vol. 35, no. 2, pp. 239–254, 1995.
- [39] V. Walsh, “Colour vision: Adapting to change,” *Current Biology*, vol. 5, no. 7, pp. 703–705, 1995.
- [40] M. A. Webster and J. Mollon, “Colour constancy influenced by contrast adaptation,” *Nature*, vol. 373, no. 6516, pp. 694–698, 1995.
- [41] R. B. Lotto and D. Purves, “The effects of color on brightness,” *Nature neuroscience*, vol. 2, no. 11, pp. 1010–1014, 1999.
- [42] T. A. Chaplin, M. G. Rosa, and L. L. Lui, “Auditory and visual motion processing and integration in the primate cerebral cortex,” *Frontiers in neural circuits*, vol. 12, p. 93, 2018.
- [43] O. Braddick, J. Atkinson, and J. Wattam-Bell, “Normal and anomalous development of visual motion processing: motion coherence and ‘dorsal-stream vulnerability’,” *Neuropsychologia*, vol. 41, no. 13, pp. 1769–1784, 2003.
- [44] A. C. Huk and D. J. Heeger, “Pattern-motion responses in human visual cortex,” *Nature neuroscience*, vol. 5, no. 1, pp. 72–75, 2002.
- [45] A. T. Smith, R. J. Snowden, and A. B. Milne, “Is global motion really based on

- spatial integration of local motion signals?," *Vision research*, vol. 34, no. 18, pp. 2425–2430, 1994.
- [46] M. Castelo-Branco, E. Formisano, W. Backes, F. Zanella, S. Neuenschwander, W. Singer, and R. Goebel, "Activity patterns in human motion-sensitive areas depend on the interpretation of global motion," *Proceedings of the National Academy of Sciences*, vol. 99, no. 21, pp. 13914–13919, 2002.
- [47] A. C. Huk, R. F. Dougherty, and D. J. Heeger, "Retinotopy and functional subdivision of human areas mt and mst," *Journal of Neuroscience*, vol. 22, no. 16, pp. 7195–7205, 2002.
- [48] S. Zeki, "Area v5—a microcosm of the visual brain," *Frontiers in integrative neuroscience*, vol. 9, p. 21, 2015.
- [49] R. F. Helfrich, H. G. Becker, and T. Haarmeier, "Processing of coherent visual motion in topographically organized visual areas in human cerebral cortex," *Brain topography*, vol. 26, no. 2, pp. 247–263, 2013.
- [50] J. Wattam-Bell, D. Birtles, P. Nyström, C. Von Hofsten, K. Rosander, S. Anker, J. Atkinson, and O. Braddick, "Reorganization of global form and motion processing during human visual development," *Current Biology*, vol. 20, no. 5, pp. 411–415, 2010.
- [51] S. Pitzalis, P. Fattori, and C. Galletti, "The human cortical areas v6 and v6a," *Visual neuroscience*, vol. 32, 2015.
- [52] C. S. Konen and S. Kastner, "Representation of eye movements and stimulus motion in topographically organized areas of human posterior parietal cortex," *Journal of Neuroscience*, vol. 28, no. 33, pp. 8361–8375, 2008.
- [53] S. Pitzalis, C. Serra, V. Sulpizio, G. Committeri, F. de Pasquale, P. Fattori, C. Galletti, R. Sepe, and G. Galati, "Neural bases of self-and object-motion in a naturalistic vision," *Human brain mapping*, vol. 41, no. 4, pp. 1084–1111, 2020.
- [54] M. J. Berry, I. H. Brivanlou, T. A. Jordan, and M. Meister, "Anticipation of moving stimuli by the retina," *Nature*, vol. 398, no. 6725, pp. 334–338, 1999.
- [55] L. Teichmann, G. Edwards, and C. I. Baker, "Resolving visual motion through perceptual gaps," *Trends in Cognitive Sciences*, vol. 25, no. 11, pp. 978–991, 2021.
- [56] J. Culham, S. He, S. Dukelow, and F. A. Verstraten, "Visual motion and the

- human brain: what has neuroimaging told us?," *Acta psychologica*, vol. 107, no. 1-3, pp. 69–94, 2001.
- [57] P. Sterzer, M. O. Russ, C. Preibisch, and A. Kleinschmidt, "Neural correlates of spontaneous direction reversals in ambiguous apparent visual motion," *Neuroimage*, vol. 15, no. 4, pp. 908–916, 2002.
- [58] Z. Kourtzi and N. Kanwisher, "Activation in human mt/mst by static images with implied motion," *Journal of cognitive neuroscience*, vol. 12, no. 1, pp. 48–55, 2000.
- [59] A. Pavan, L. F. Cuturi, M. Maniglia, C. Casco, and G. Campana, "Implied motion from static photographs influences the perceived position of stationary objects," *Vision research*, vol. 51, no. 1, pp. 187–194, 2011.
- [60] S. He, E. R. Cohen, and X. Hu, "Close correlation between activity in brain area mt/v5 and the perception of a visual motion aftereffect," *Current Biology*, vol. 8, no. 22, pp. 1215–1218, 1998.
- [61] G. Rees, K. Friston, and C. Koch, "A direct quantitative relationship between the functional properties of human and macaque v5," *Nature neuroscience*, vol. 3, no. 7, pp. 716–723, 2000.
- [62] R. Blake, R. Sekuler, and E. Grossman, *The Primate Visual System*. CRC Press, 2003.
- [63] M. Castelo-Branco, R. Goebel, S. Neuenschwander, and W. Singer, "Neural synchrony correlates with surface segregation rules," *Nature*, vol. 405, no. 6787, pp. 685–689, 2000.
- [64] L. R. Kozak and M. Castelo-Branco, "Peripheral influences on motion integration in foveal vision are modulated by central local ambiguity and center-surround congruence," *Investigative ophthalmology & visual science*, vol. 50, no. 2, pp. 980–988, 2009.
- [65] M. Castelo-Branco, L. R. Kozak, E. Formisano, J. Teixeira, J. Xavier, and R. Goebel, "Type of featural attention differentially modulates hmt+ responses to illusory motion aftereffects," *Journal of neurophysiology*, vol. 102, no. 5, pp. 3016–3025, 2009.
- [66] M. Wertheimer, "Experimentelle studien uber das sehen von bewegung," *Zeitschrift fur psychologie*, vol. 61, 1912.
- [67] N. Van Humber, T. Putzeys, and J. Wagemans, "Apparent motion sup-

- presses responses in early visual cortex: a population code model,” *PLoS computational biology*, vol. 12, no. 10, p. e1005155, 2016.
- [68] P. A. Kolars and M. von Grünau, “Shape and color in apparent motion,” *Vision research*, vol. 16, no. 4, pp. 329–335, 1976.
- [69] S. Hidaka, M. Nagai, A. B. Sekuler, P. J. Bennett, and J. Gyoba, “Inhibition of target detection in apparent motion trajectory,” *Journal of Vision*, vol. 11, no. 10, pp. 2–2, 2011.
- [70] H. Hogendoorn, T. A. Carlson, and F. A. Verstraten, “Interpolation and extrapolation on the path of apparent motion,” *Vision research*, vol. 48, no. 7, pp. 872–881, 2008.
- [71] S. Yantis and T. Nakama, “Visual interactions in the path of apparent motion,” *Nature neuroscience*, vol. 1, no. 6, pp. 508–512, 1998.
- [72] R. Goebel, D. Khorram-Sefat, L. Muckli, H. Hacker, and W. Singer, “The constructive nature of vision: direct evidence from functional magnetic resonance imaging studies of apparent motion and motion imagery,” *European Journal of Neuroscience*, vol. 10, no. 5, pp. 1563–1573, 1998.
- [73] L. Muckli, N. Kriegeskorte, H. Lanfermann, F. E. Zanella, W. Singer, and R. Goebel, “Apparent motion: event-related functional magnetic resonance imaging of perceptual switches and states,” *Journal of Neuroscience*, vol. 22, no. 9, pp. RC219–RC219, 2002.
- [74] P. Vetter, M.-H. Grosbras, and L. Muckli, “Tms over v5 disrupts motion prediction,” *Cerebral cortex*, vol. 25, no. 4, pp. 1052–1059, 2015.
- [75] M. Hurme, M. Koivisto, A. Revonsuo, and H. Railo, “V1 activity during feedforward and early feedback processing is necessary for both conscious and unconscious motion perception,” *NeuroImage*, vol. 185, pp. 313–321, 2019.
- [76] C. A. Pedersini, A. Lingnau, N. Cardobi, J. Sanchez-Lopez, S. Savazzi, and C. A. Marzi, “Neural bases of visual processing of moving and stationary stimuli presented to the blind hemifield of hemianopic patients,” *Neuropsychologia*, vol. 141, p. 107430, 2020.
- [77] J. Silvanto, A. Cowey, N. Lavie, and V. Walsh, “Striate cortex (v1) activity gates awareness of motion,” *Nature neuroscience*, vol. 8, no. 2, pp. 143–144, 2005.
- [78] A. Larsen, K. H. Madsen, T. E. Lund, and C. Bundesen, “Images of illusory

- motion in primary visual cortex,” *Journal of cognitive neuroscience*, vol. 18, no. 7, pp. 1174–1180, 2006.
- [79] L. Muckli, A. Kohler, N. Kriegeskorte, and W. Singer, “Primary visual cortex activity along the apparent-motion trace reflects illusory perception,” *PLoS biology*, vol. 3, no. 8, p. e265, 2005.
- [80] B. Ahmed, A. Hanazawa, C. Undeman, D. Eriksson, S. Valentinienė, and P. E. Roland, “Cortical dynamics subserving visual apparent motion,” *Cerebral Cortex*, vol. 18, no. 12, pp. 2796–2810, 2008.
- [81] M. Wibral, C. Bledowski, A. Kohler, W. Singer, and L. Muckli, “The timing of feedback to early visual cortex in the perception of long-range apparent motion,” *Cerebral cortex*, vol. 19, no. 7, pp. 1567–1582, 2009.
- [82] P. Sterzer, J.-D. Haynes, and G. Rees, “Primary visual cortex activation on the path of apparent motion is mediated by feedback from hmt+/v5,” *Neuroimage*, vol. 32, no. 3, pp. 1308–1316, 2006.
- [83] K. Friston, “A theory of cortical responses,” *Philosophical transactions of the Royal Society B: Biological sciences*, vol. 360, no. 1456, pp. 815–836, 2005.
- [84] R. P. Rao and D. H. Ballard, “Predictive coding in the visual cortex: a functional interpretation of some extra-classical receptive-field effects,” *Nature neuroscience*, vol. 2, no. 1, pp. 79–87, 1999.
- [85] G. Edwards, P. Vetter, F. McGruer, L. S. Petro, and L. Muckli, “Predictive feedback to v1 dynamically updates with sensory input,” *Scientific reports*, vol. 7, no. 1, pp. 1–12, 2017.
- [86] A. Alink, C. M. Schwiedrzik, A. Kohler, W. Singer, and L. Muckli, “Stimulus predictability reduces responses in primary visual cortex,” *Journal of Neuroscience*, vol. 30, no. 8, pp. 2960–2966, 2010.
- [87] L. M. Harrison, K. E. Stephan, G. Rees, and K. J. Friston, “Extra-classical receptive field effects measured in striate cortex with fmri,” *Neuroimage*, vol. 34, no. 3, pp. 1199–1208, 2007.
- [88] R. Sekuler, “Motion perception: A modern view of wertheimer’s 1912 monograph,” *Perception*, vol. 25, no. 10, pp. 1243–1258, 1996.
- [89] P. von Schiller, “Stroboskopischen alternativbewegungen [stroboscopic alternative motion],” *Psychologische Forschung*, vol. 17, pp. 179–214, 1933.



- 
- [90] A. Chaudhuri and D. A. Glaser, “Metastable motion anisotropy,” *Visual neuroscience*, vol. 7, no. 5, pp. 397–407, 1991.
- [91] R. Blake and N. K. Logothetis, “Visual competition,” *Nature Reviews Neuroscience*, vol. 3, no. 1, pp. 13–21, 2002.
- [92] Y. Weiss, E. P. Simoncelli, and E. H. Adelson, “Motion illusions as optimal percepts,” *Nature neuroscience*, vol. 5, no. 6, pp. 598–604, 2002.
- [93] J. Kornmeier, C. M. Hein, and M. Bach, “Multistable perception: when bottom-up and top-down coincide,” *Brain and cognition*, vol. 69, no. 1, pp. 138–147, 2009.
- [94] E. Chiappini, A. Sel, P. B. Hibbard, A. Avenanti, and V. Romei, “Increasing interhemispheric connectivity between human visual motion areas uncovers asymmetric sensitivity to horizontal motion,” *Current Biology*, 2022.
- [95] S. Liu, P. U. Tse, and P. Cavanagh, “Meridian interference reveals neural locus of motion-induced position shifts,” *Journal of Neurophysiology*, vol. 119, no. 6, pp. 2091–2099, 2018.
- [96] T. A. Carlson, G. A. Alvarez, and P. Cavanagh, “Quadrantic deficit reveals anatomical constraints on selection,” *Proceedings of the National Academy of Sciences*, vol. 104, no. 33, pp. 13496–13500, 2007.
- [97] D. G. Pelli, “Crowding: A cortical constraint on object recognition,” *Current opinion in neurobiology*, vol. 18, no. 4, pp. 445–451, 2008.
- [98] D. H. Brainard and S. Vision, “The psychophysics toolbox,” *Spatial vision*, vol. 10, no. 4, pp. 433–436, 1997.
- [99] A. Kohler, L. Haddad, W. Singer, and L. Muckli, “Deciding what to see: The role of intention and attention in the perception of apparent motion,” *Vision research*, vol. 48, no. 8, pp. 1096–1106, 2008.
- [100] Z.-L. Lu and B. Doshier, *Visual psychophysics*. The MIT Press, London, England: MIT Press, Oct. 2013.
- [101] W. H. Ehrenstein and A. Ehrenstein, “Psychophysical methods,” in *Modern techniques in neuroscience research*, pp. 1211–1241, Springer, 1999.
- [102] N. Prins *et al.*, *Psychophysics: a practical introduction*. Academic Press, 2010.
- [103] F. A. Wichmann and N. J. Hill, “The psychometric function: I. fitting,

- sampling, and goodness of fit,” *Perception & psychophysics*, vol. 63, no. 8, pp. 1293–1313, 2001.
- [104] F. W. Cornelissen, E. M. Peters, and J. Palmer, “The eyelink toolbox: eye tracking with matlab and the psychophysics toolbox,” *Behavior Research Methods, Instruments, & Computers*, vol. 34, no. 4, pp. 613–617, 2002.
- [105] G. Avidan, M. Harel, T. Hendler, D. Ben-Bashat, E. Zohary, and R. Malach, “Contrast sensitivity in human visual areas and its relationship to object recognition,” *Journal of neurophysiology*, vol. 87, no. 6, pp. 3102–3116, 2002.
- [106] G. M. Boynton, J. B. Demb, G. H. Glover, and D. J. Heeger, “Neuronal basis of contrast discrimination,” *Vision research*, vol. 39, no. 2, pp. 257–269, 1999.
- [107] D. Ress and D. J. Heeger, “Neuronal correlates of perception in early visual cortex,” *Nature neuroscience*, vol. 6, no. 4, pp. 414–420, 2003.
- [108] J. Gengerelli, “Apparent movement in relation to homonymous and heteronymous stimulation of the cerebral hemispheres.,” *Journal of Experimental Psychology*, vol. 38, no. 5, p. 592, 1948.
- [109] S. Ullman, *The interpretation of visual motion*. Massachusetts Inst of Technology Pr, 1979.
- [110] G. S. Masson and U. J. Ilg, *Dynamics of visual motion processing*. Springer, 2010.
- [111] D. Burr and P. Thompson, “Motion psychophysics: 1985–2010,” *Vision research*, vol. 51, no. 13, pp. 1431–1456, 2011.
- [112] M. Shimono, H. Mano, and K. Niki, “The brain structural hub of interhemispheric information integration for visual motion perception,” *Cerebral cortex*, vol. 22, no. 2, pp. 337–344, 2012.
- [113] S. O. Dumoulin, C. L. Baker, and R. F. Hess, “Centrifugal bias for second-order but not first-order motion,” *JOSA A*, vol. 18, no. 9, pp. 2179–2189, 2001.
- [114] C. W. Clifford, D. J. Mannion, and J. S. McDonald, “Radial biases in the processing of motion and motion-defined contours by human visual cortex,” *Journal of neurophysiology*, vol. 102, no. 5, pp. 2974–2981, 2009.
- [115] M. Raemaekers, M. J. Lankheet, S. Moorman, Z. Kourtzi, and R. J. Van Wezel,

- “Directional anisotropy of motion responses in retinotopic cortex,” *Human brain mapping*, vol. 30, no. 12, pp. 3970–3980, 2009.
- [116] R. T. Maloney, T. L. Watson, and C. W. Clifford, “Determinants of motion response anisotropies in human early visual cortex: The role of configuration and eccentricity,” *NeuroImage*, vol. 100, pp. 564–579, 2014.
- [117] E. H. Silson, R. C. Reynolds, D. J. Kravitz, and C. I. Baker, “Differential sampling of visual space in ventral and dorsal early visual cortex,” *Journal of Neuroscience*, vol. 38, no. 9, pp. 2294–2303, 2018.
- [118] G. Lerma-Usabiaga, J. Winawer, and B. A. Wandell, “Population receptive field shapes in early visual cortex are nearly circular,” *Journal of Neuroscience*, vol. 41, no. 11, pp. 2420–2427, 2021.
- [119] L. Spillmann and J. S. Werner, “Long-range interactions in visual perception,” *Trends in neurosciences*, vol. 19, no. 10, pp. 428–434, 1996.
- [120] B. Le Bec, X. G. Troncoso, C. Desbois, Y. Passarelli, P. Baudot, C. Monier, M. Pananceau, and Y. Frégnac, “Horizontal connectivity in v1: Prediction of coherence in contour and motion integration,” *Plos one*, vol. 17, no. 7, p. e0268351, 2022.
- [121] S. Chemla, A. Reynaud, M. Di Volo, Y. Zerlaut, L. Perrinet, A. Destexhe, and F. Chavane, “Suppressive traveling waves shape representations of illusory motion in primary visual cortex of awake primate,” *Journal of Neuroscience*, vol. 39, no. 22, pp. 4282–4298, 2019.





A

# Appendix

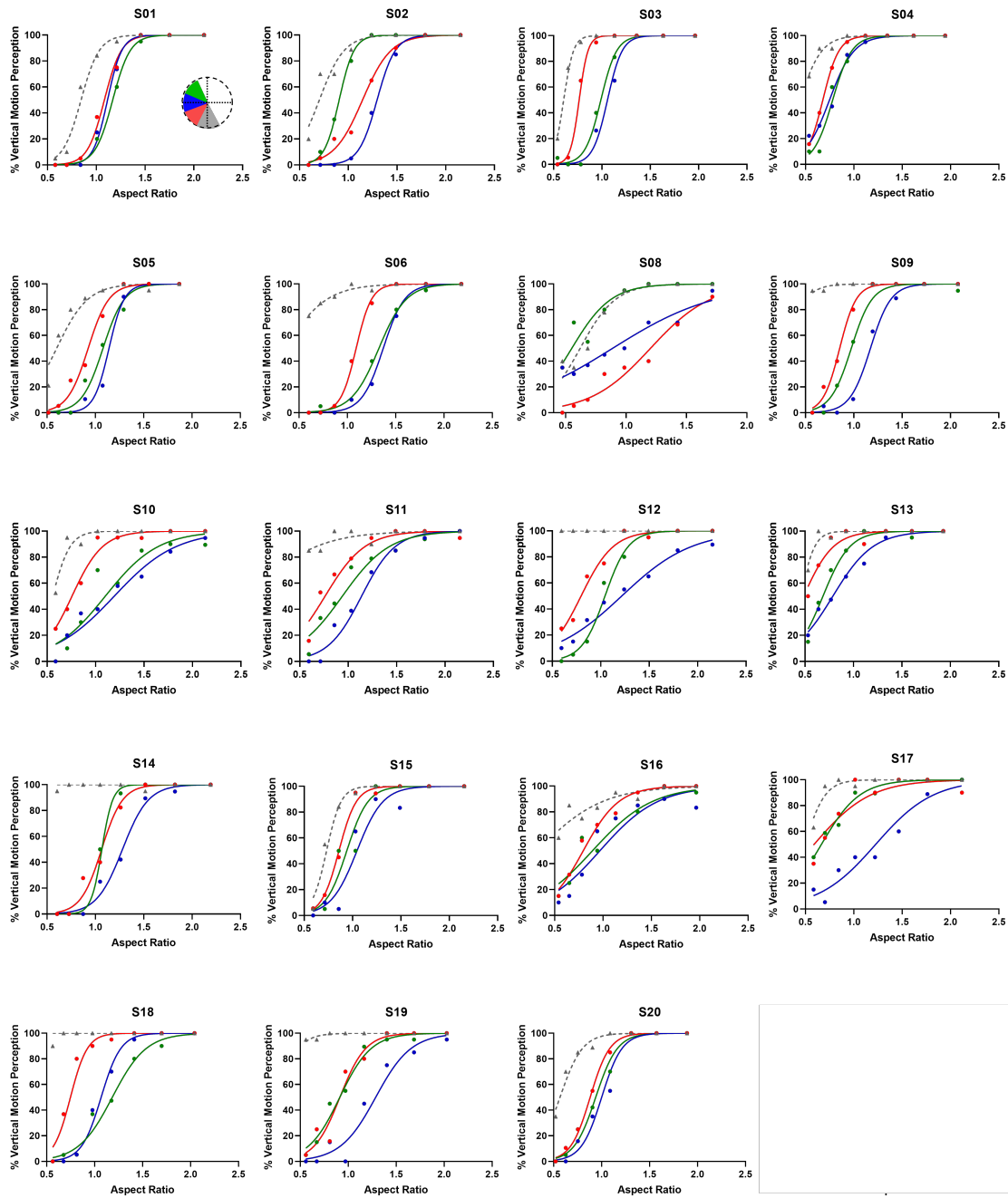


**Figure A.1: Psychometric functions for the left hemifield of all participants in experiment 1.** The psychometric fits represent the percentage of vertical motion perception relatively to the aspect ratio. Dots correspond to the 8 aspect ratios used during Method of Constant Stimuli (MoCS) task. Blue color represents the middle position ( $180^\circ$ ), the green color corresponds to top ( $135^\circ$ ), the red color represents the bottom position ( $225^\circ$ ) and the gray color corresponds to control position ( $270^\circ$ ).

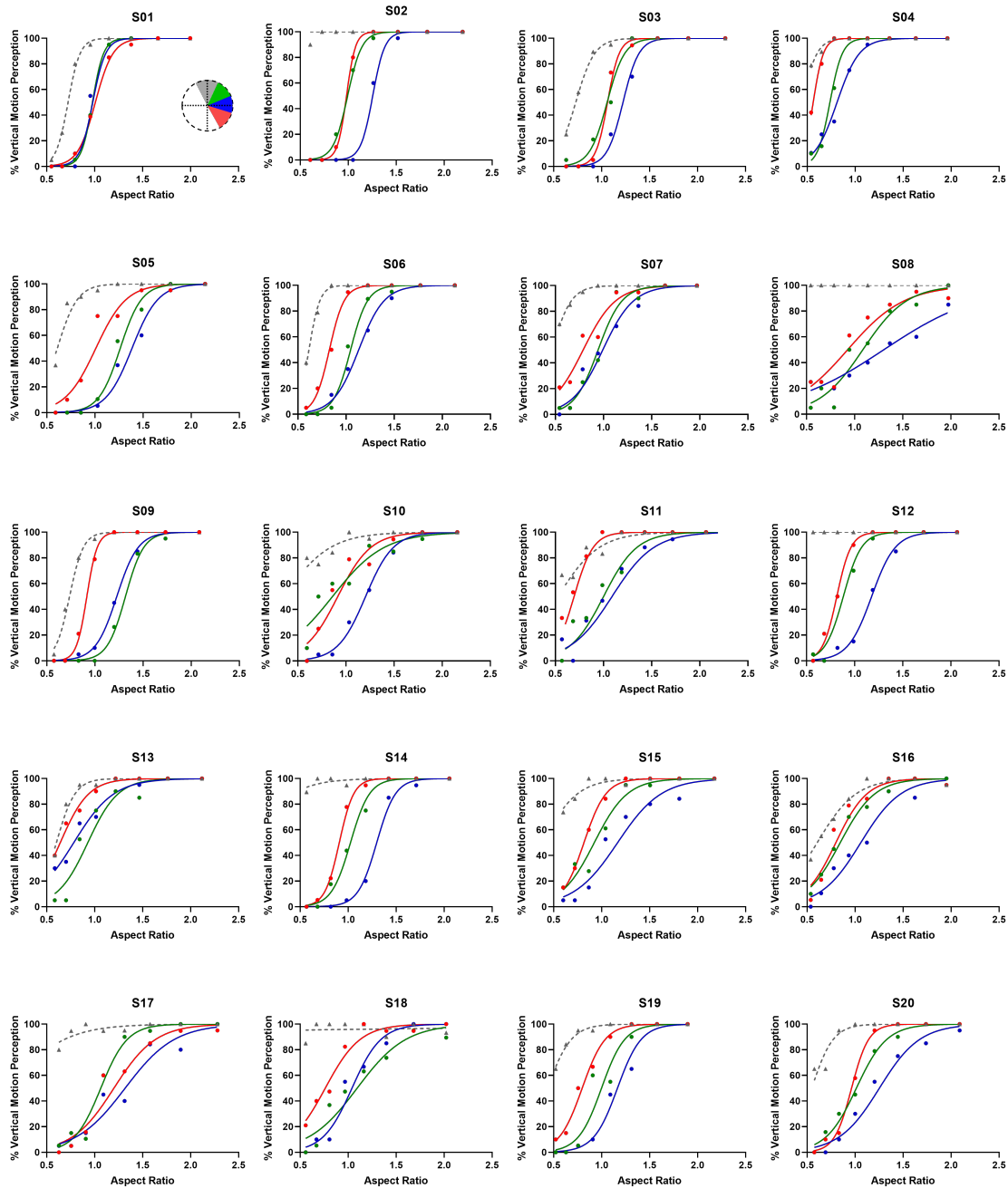


**Figure A.2: Psychometric functions for the right hemifield of all participants in experiment 1.** The psychometric fits represent the percentage of vertical motion perception relatively to the aspect ratio. Dots correspond to the 8 aspect ratios used during MoCS task. Blue color represents the middle position ( $0^\circ$ ), the green color corresponds to top position ( $45^\circ$ ), the red color represents the bottom position ( $315^\circ$ ) and the gray color corresponds to control position ( $90^\circ$ ).



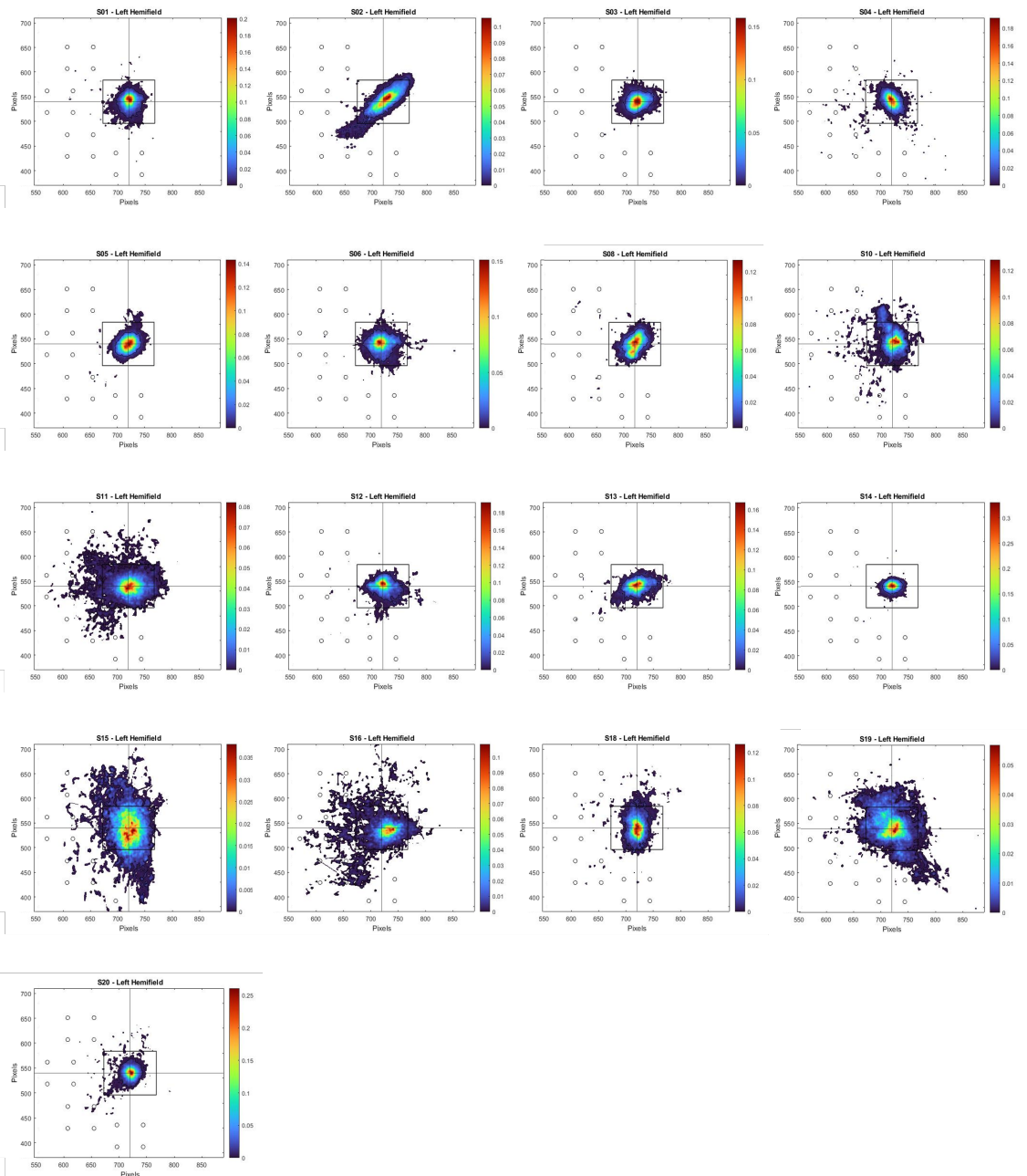


**Figure A.3:** Average fixation density plots for the left hemifield of all participants. The screen's centre is given by the intersection of axes  $y = 1080/2$  px and  $x = 1440/2$  px. The window's dimensions, at the centre of the plots, are described in section 3.5.2. The black contour contains 90% of the gaze position data. Black circles represent the stimulus' positions during the visual task.

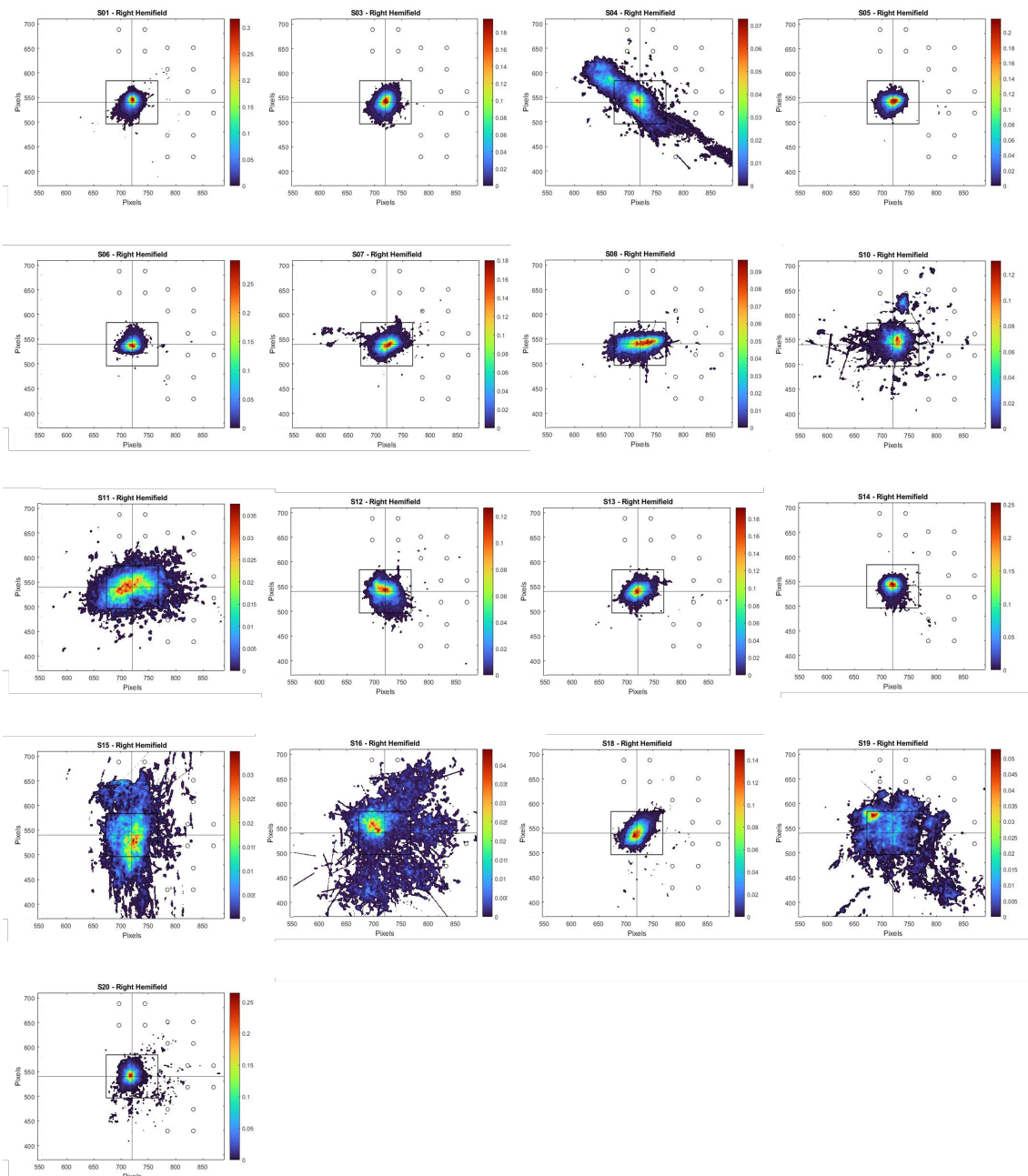


**Figure A.4: Average fixation density plots for the right hemifield of all participants.** The screen's centre is given by the intersection of axes  $y = 1080/2$  px and  $x = 1440/2$  px. The window's dimensions, at the centre of the plots, are described in section 3.5.2. The black contour contains 90% of the gaze position data. Black circles represent the stimulus' positions during the visual task.

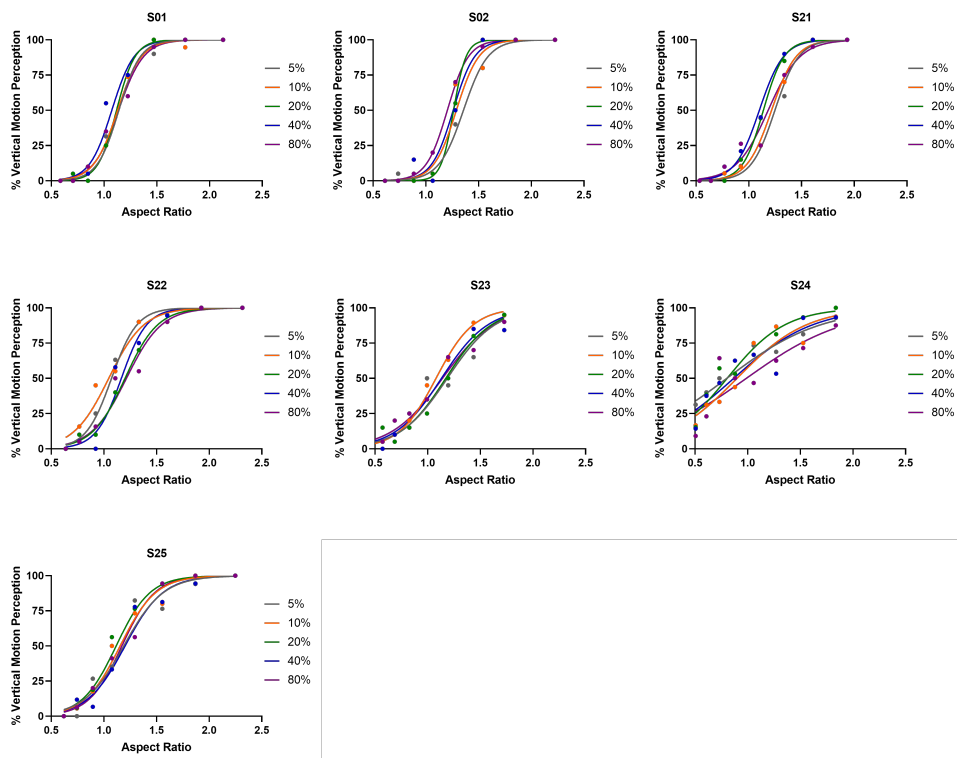


**Figure A.5: Psychometric functions for all participants in experiment 2.** The psychometric fits represent the percentage of vertical motion perception in relation to the aspect ratio. The colored dots are the 8 aspect ratios used during MoCS task. The five different colors corresponds to the 5 levels of Michelson contrast percentages.